TSX™ IMPLANT

Designed for Enhanced Primary Stability and Peri-Implant Health

Author
Elnaz Ajami, MSc, PhD

ZimVie

Master's Degree – Clinical Engineering
University of Liverpool, UK

PhD – Biomaterials Science & Engineering,
University of London, UK

Author

Elnaz Ajami, MSc, PhD

Table of Contents

The increased prevalence of peri-implantitis and demand for immediacy protocols were the two main rationales behind ZimVie's new TSX Implant design.

When designing the TSX Implant, the primary focus was to create an aggressive thread profile with wider thread crests that cut deeper into the osteotomy wall compared to traditional Tapered Screw-Vent® (TSV®) Implants. This resulted in an increased initial engagement of the implant with the surrounding bone and high primary stability as well as improved apical stability following immediate placement in fresh extraction sockets.[1] In doing so, it was ensured that the threads were not overly aggressive. Threads which are too aggressive could result in a self-driving implant with a propensity to shift off axis while being placed in the osteotomy, leading to a risk of implant placement too close to the buccal or lingual walls.

When designing the TSX Implant's coronal region, platform switching was incorporated,[2-14] and an established friction-fit internal hex connection was chosen for implant-abutment stability[15-20] and to maintain crestal bone levels and long-term peri-implant tissue health. In addition, a contemporary hybrid surface with long-term clinical evidence was chosen *(Figure 1)*.

The coronal surface of the implant has been textured with a dual acid etching technology (i.e. Osseotite®) – a surface with over 20 years of proven clinical success.[21-27] This surface provides improved osteoconductive potential for crestal bone maintenance compared to a traditional machined collar [28-31] while minimizing bacterial adhesion to the level of machined surfaces,[32-34] lowering one of the risk factors associated with peri-implantitis.[35]

Furthermore, in the unlikely event of surface exposure and contamination, minimally rough coronal surfaces may be cleaned more easily than rougher surface topographies. Lastly, for texturing of the subcoronal region, the grit-blasted surface of the predicate TSV Implant (i.e. MTX™), which also has proven clinical success over two decades, is utilized.[36, 37]

Fig. 1

TSX Implant with Contemporary Hybrid Surface.

The **TSX Implant** incorporates several design elements with a long history of clinical use established by Screw-Vent® and TSV Implants. The origins of these design features and understanding of their clinical rationale and evidence provide historical context for the evolution of the TSX Implant.

In 1991, the U.S. Department of Veterans Affairs (VA) launched a prospective multi-center study to determine the influence of implant design and bone location on long-term implant success.

A straight-body implant (Screw-Vent), which was first introduced in 1986 with a cpTi Branemark-style thread, was one of the four implant designs selected for the study. The VA study comprised more than 800 patients, a total of 2,795 implants, and over 80 investigators at 30 VA medical centers and two university dental schools.[38]

Based on the results of the VA study, the design, material, surface and surgical protocol of the Screw-Vent implant were subsequently improved, resulting in the introduction of the TSV Implant to better address the differing requirements of hard and soft bone. Several of those TSV design features were incorporated into the TSX Implant today: a tapered body, a multi-lead thread, the original friction-fit internal hex connection, soft and dense bone drilling protocols, and a new hybrid surface design with a minimally rough collar and higher roughness on the implant body.

Several design elements were incorporated into the **TSX Implant** design to facilitate immediacy protocols, crestal bone preservation, and peri-implant health.

TSX Design for Primary Stability

The new TSX Implant includes unique design features to enhance implant primary stability by increasing the surface area of the implant that comes into initial contact with bone and providing a progressive increase of torque as the implant is inserted. This will help achieve high stability and sufficient insertion torque to instill confidence from tactile feel of stability during placement while not generating excessive insertion torque values.[1]

The TSX Implant has a contemporary tapered design with progressively increased thread depths that result in more apical taper at the implant's minor *(yellow line Figure 2)* than major diameter *(red line- Figure 2)* compared to TSV. For the apical region of a 4.7mm x 13mm implant, the taper of TSX is measured 6º compared to 5º of TSV, and the apical thread depth of TSX is measured 0.64mm compared to 0.35mm of TSV *(Figure 2)*. TSX Implants are aggressive, yet the self-tapping TSX Implant macrogeometry does not drift during the placement and follows the shape of the drilled osteotomy, thus designed to stay on course during seating, aiding in placement predictability.[1]

The newly designed aggressive threads penetrate deep into the bone, which in combination with the removal of apical vent present in the TSV Implant, increases the surface area of the implant that comes in contact with bone at the time of implant placement (i.e. IBIC), thus providing increased apical implant stability.[1] Additionally, the new design allows the implant to achieve high primary stability in fresh extraction sockets and in the sites with irregular shapes. The implant is introduced with a wide range of diameters, including 3.1mm and 5.4mm, and soft and dense bone drilling protocols, with the addition of an extraction protocol, and thus can be placed in all bone types and any alveolar location.[1] The TSX Implant may be placed at bone level or slightly below the bone crest according to clinical situation and preference.[1] The new TSX Implant thread pattern has changed from the triple-lead of TSV to a double-lead in order to accommodate the space needed for aggressive thread design without resulting in extremely high torque values.[1]

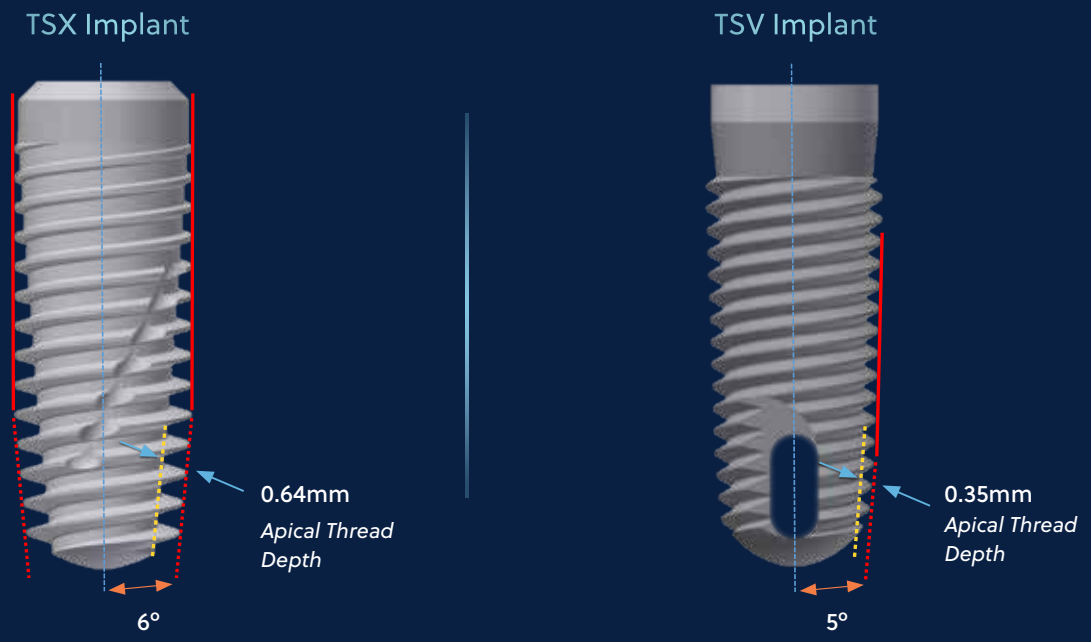

Fig. 2 *CAD model of (left) TSX 4.7mm x 13mm and (right) TSV 4.7mm x 13mm. The yellow lines show the minor diameter taper and the red lines show the major diameter taper. The blue arrows point at the depth of the threads.*

TSX Primary Stability Test Methods

Primary stability of the TSX Implant compared to the traditional TSV Implant system has been assessed with insertion torque and ISQ measurements as well bone-to-implant contact at placement (IBIC) at dense and soft bone following full, apical, and extraction protocols as described below.

Full Placement Protocol: Insertion Torque and ISQ Measurements

For testing in a traditional osteotomy, a strip of 50/30 simulated bone block (sawbone) was used, representing a dense bone structure. A drill press was used for all drilling steps to ensure an accurate osteotomy creation. The osteotomies were created using dense bone drilling protocol per chosen diameter and length, as shown in *(Figure 3).* No bone tap was utilized, creating a worst-case scenario for dense bone placement.

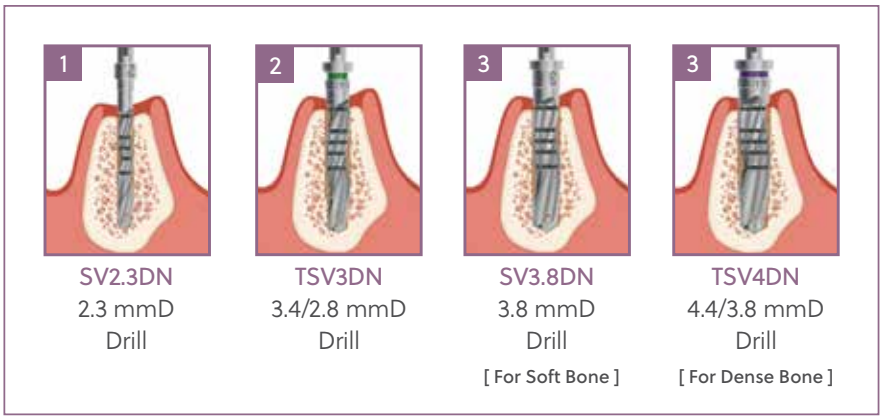

Fig. 3 *Standard drilling protocol for TSX and TSV 4.7mmD.*

Soft bone drilling protocol was followed for placing TSX Implants in soft bone with a strip of 40/20 simulated bone block (sawbone) representing a soft bone structure. When creating the osteotomy, the soft bone drilling protocol *(Figure 3)* was utilized on the porous (20 PCF) side.

For ISQ measurements in dense bone, the respective SmartPegs were hand-tightened to the implant using a SmartPeg Mount. The Osstell wand was placed perpendicular to the implant at four spots approximately 90° apart *(Figure 4, green arrows).* The ISQ values were recorded at all four locations.

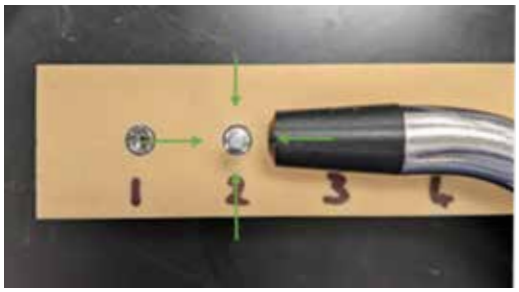

Fig.4

ISQ Measurement Using Osstell device. *The green arrows show the direction of the wand at four locations approximately 90° apart around the SmartPeg connected to the implant.*

Apical Placement Protocol: Insertion Torque Measurements

Apical placement protocol is used to mimic the position of implants in fresh extraction sockets in a worst-case scenario in which only the apical 4mm portion of the implant engages with bone while the coronal portion and most of the implant mid-section are not in contact with the bony wall *(Figure 5)*. For this protocol, a strip of 50/30 bone block (sawbone) was used, representing a dense bone structure, although apical implant contact occurred primarily or entirely in 30 PCF sawbone simulating a medium-to soft density. A drill press was used for all drilling steps to ensure an accurate osteotomy creation. The osteotomies were created using EZT28D24G (2.8mm/2.4mm Step Drill), TSV3.4DN (3.4mm/2.8mm Step Drill), TSV3.8DN (3.8mm/3.4mm Step Drill), TSV4DN (4.4mm/3.8mm Step Drill), TSV5.1DN (5.1mm/4.4mm Step Drill), or TSV6DN (5.7mm/5.1mm Step Drill) to full depth at varying lengths of 8, 10, 11.5, 13 and 16mm to place TSX and TSV Implants of 3.1, 3.7, 4.1, 4.7, 5.4, or 6.0mm diameters. Finally, a drill larger than the diameter of the preceding drill was used to open coronal and middle of the osteotomy to provide engagement with bone only for the remainder 4mm apical portion of the implant when placed *(Figure 5)*.

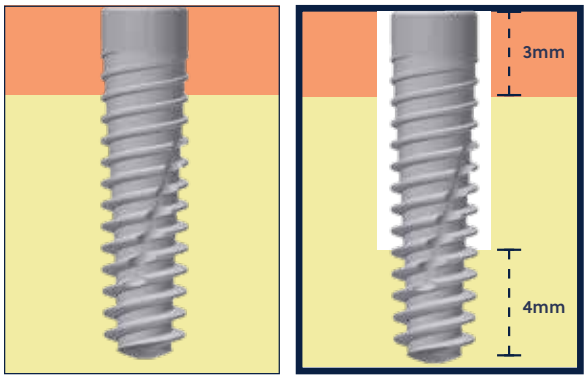

Fig. 5

An illustration of the full vs. apical only engagement of the implant in the bone. The top 3mm in orange color is the cortical plate simulated by 50 PCF bone block. In the apical engagement shown on the right, only the bottom 4mm of the implant is engaged with the medium-to-soft 30 PCF bone block, whereas on the left side image (full insertion), the whole implant is engaging with bone coronal to apical.

The apical placement extraction protocol mimics undersized osteotomy scenarios for fresh extraction sockets. For this protocol, the same protocol was followed as for apical placement above, except the osteotomies were created using SV2.3DN (2.3mm Twist Drill), SV2.3DN (2.3mm Twist Drill), SV2.8DN (2.8mm Twist Drill), SV3.4DN (3.4mm Twist Drill) to place TSX Implants with 3.1, 3.7, 4.1, or 4.7mm diameters, respectively, at full depth at varying lengths. Osteotomies for TSV Implants were created using the same drills as used in the aforementioned apical placement protocol, since TSV Implants are not indicated for use in undersized osteotomies. For 5.4mm and 6.0mm diameter TSX and TSV Implants, the extraction protocol followed the same drilling sequence as above (i.e. TSV5.1DN (5.1mm / 4.4mm Step Drill), or TSV6DN (5.7mm / 5.1mm Step Drill), respectively, in order to avoid very high placement torque values above 100 N.cm that cannot be measured and assessed with a torque-indicating ratchet wrench such as ZTIRW. Thus, the apical placement extraction protocol for 5.4mm and 6.0mm TSX Implants and TSV Implants is identical.

To measure the apical insertion torque, the bone strip was attached to a fixture *(Figure 6a)*, ensuring that it was adequately tightened and that the hole being used was centered in the fixture. The implant driver was then attached to the implant along with a hand wrench *(Figure 6b)*. The implant was then driven into the bone strip until it was seated crestally. The maximum torque value was recorded.

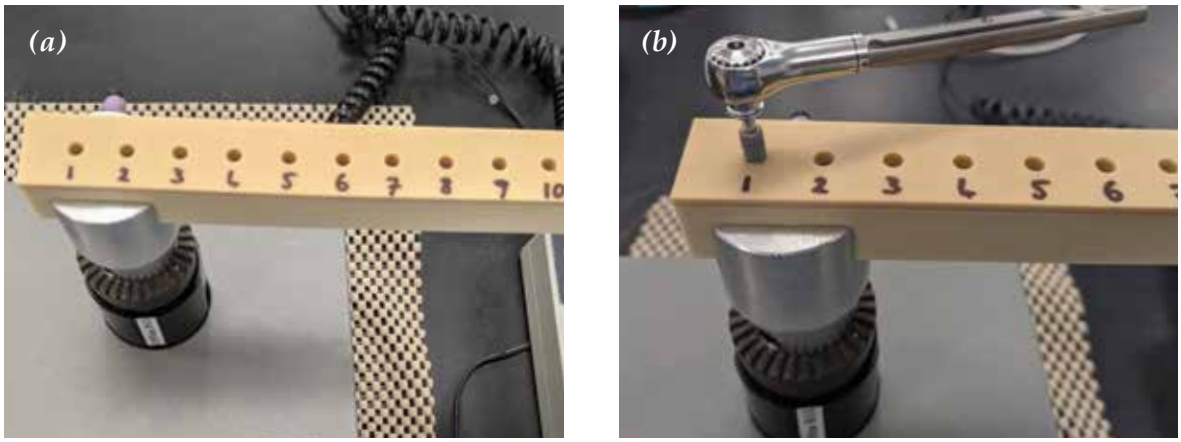

Fig. 6 *(a) Bone strip in torque fixture.* *(b) Placing implant into a bone strip.*

Full Placement Protocol: Initial Bone-to-Implant Contact Measurements

Traditional measurements of percentage bone-to-implant contact involve quantitative examination of histologic cross-sections. In this approach, a three-dimensional computer rendition of the implant and osteotomy was used to calculate IBIC% (initial bone-to-implant contact at placement).

For surface area measurements, CAD modeling software (Autodesk Inventor 2022) was utilized to collect representative surface area contact between the implant and the surrounding bone at initial implant placement, under full and apical engagement conditions. For the measurements, implant models were imported into Inventor and a model of the osteotomy was created using dimensions of the final drill in each implant's respective drilling protocol. For all models, the osteotomy (drill tip) was positioned 1.25mm beyond the apex of the implant, with the implant placed at bone level.

For full placement measurements, the implant model was placed into the osteotomy model at bone level *(Figure 7a)*. The two solids were combined to show the area of the implant in contact with the surrounding bone *(Figure 7b)*. The area measurement calculated the internal and external surface area of the implant in contact with the surrounding bone. Next, surface areas of the implant not in contact with the surrounding bone were calculated. These areas include the implant platform and collar *(Figure 7c)* and the surface area of the internal portion of the implant *(Figure 7d)*. The surface areas of the implant not in contact with bone was then subtracted from the initial area measurement to determine the surface area of the implant in contact with bone. To normalize the surface area of the implant in contact with bone, the surface area of the implant model as a solid was measured *(Figure 7e)*. Next, the surface area of the top face and bevel were calculated *(Figure 7f)* and subtracted from the solid implant measurement to yield the total surface area of the implant available to contact bone. Percent bone-to-implant contact at initial placement was calculated by dividing the external implant surface area in contact with bone by the total surface area of the implant available to contact bone and multiplying by 100.

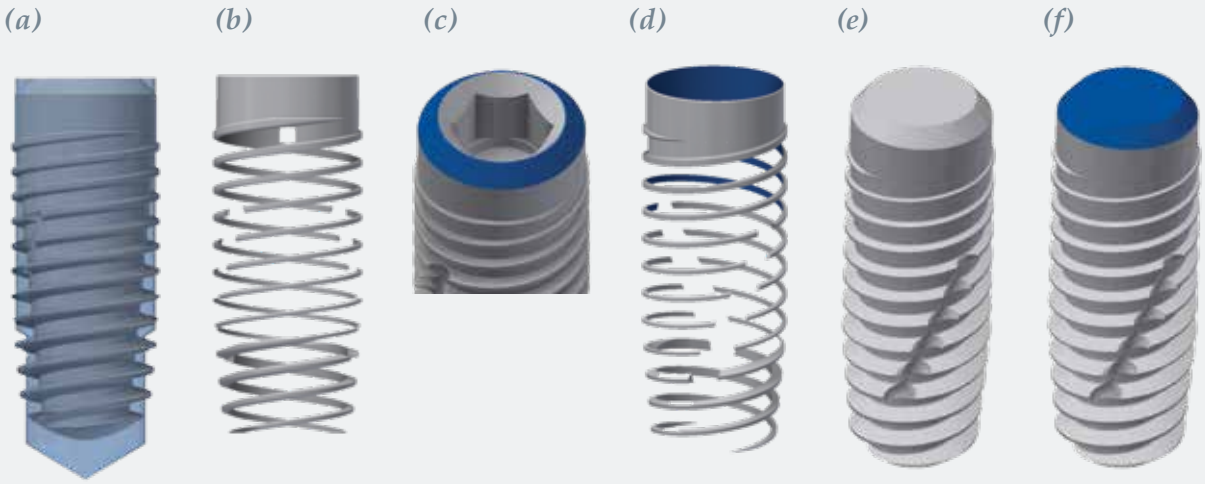

Steps of IBIC measurement in full placement protocol using the CAD modeling software.

Fig. 7 *(a) Implant in osteotomy. (b) Surface area of the implant in contact with bone. (c) Areas of the implant not in contact with bone. (d) Surface area of the internal part of implant. (e) Surface area of the implant as a solid model. (f) Surface area of top surface and bevel.*

Apical Placement Protocol: Initial Bone-to-Implant Contact Measurements

For apical placement measurements, the same method followed as described above, except that after the implant model was placed into the osteotomy model at bone the two solids were combined and the bottom 5.25mm of the resultant model was used for analysis, which provided 4mm of the implant available to contact bone for apical engagement *(Figure 8a, 8b, 8c, 8d, 8e).*

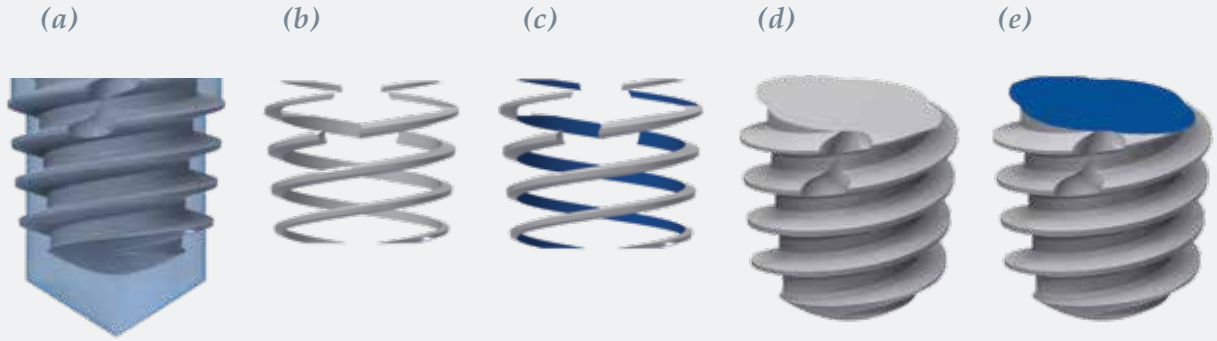

Steps of IBIC measurement in apical placement protocol using the CAD modeling software.

Fig. 8 *(a) Implant apex in osteotomy. (b) Surface area of the implant apex in contact with bone. (c) Surface area of the internal part of implant. (d) Surface area of the implant as a solid model. (e) Surface area of top surface and bevel.*

TSX Primary Stability Test Results

This section includes a summary of all the test results obtained for insertion torque, ISQ, and IBIC using different placement protocols: **(1) full placement in dense bone, (2) apical placement in dense bone, (3) apical placement using extraction protocols in dense bone, and (4) full placement in soft bone.**

Full Placement Protocol: Insertion Torque Data

The average peak insertion torque of TSX Implants is equal to or lower than the TSV Implants across different diameters when averaged across all the tested implant lengths *(Figure 9)*. This is in line with the aim to lower the insertion torque values to below 100 N.cm and achieve similar primary stability via an increase in IBIC.[1]

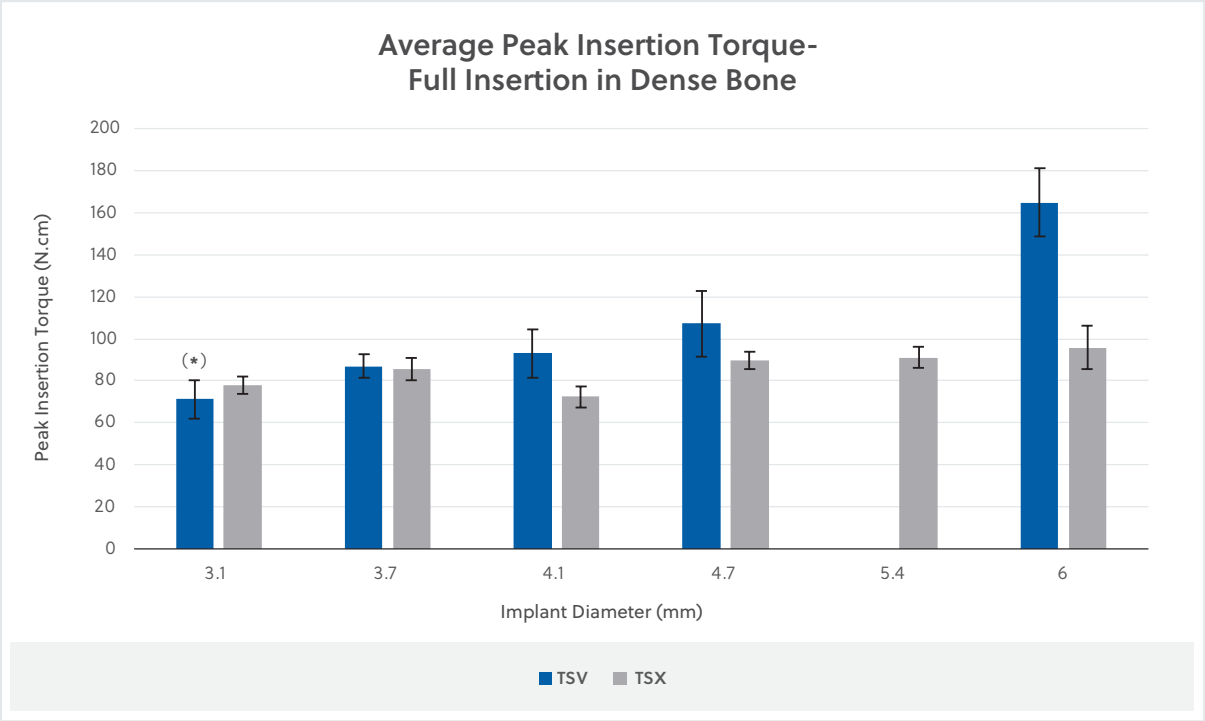

Fig. 9 *Peak insertion torque data measured for TSV and TSX Implants placed following full placement protocol in dense bone with diameters varying from 3.1mm to 6mm at varying lengths of 8.0mm to 16mm. Data from different implant lengths have been averaged for a given diameter. NOTE: The 5.4mm diameter does not exist in the TSV Implant line.*

(*) There is no 3.1mm TSV, Data is from the 3.1mm Eztetic Implant.

To take a more detailed look at the insertion torque data across different implant lengths for a given diameter, the 4.7mm implant diameter was chosen at varying lengths of 8, 10, 11.5, 13, and 16mm.

The peak insertion torque data for TSX was lower than TSV, although still in a moderate to high range, except for the 8mm where no differences were observed *(Figure 10).*

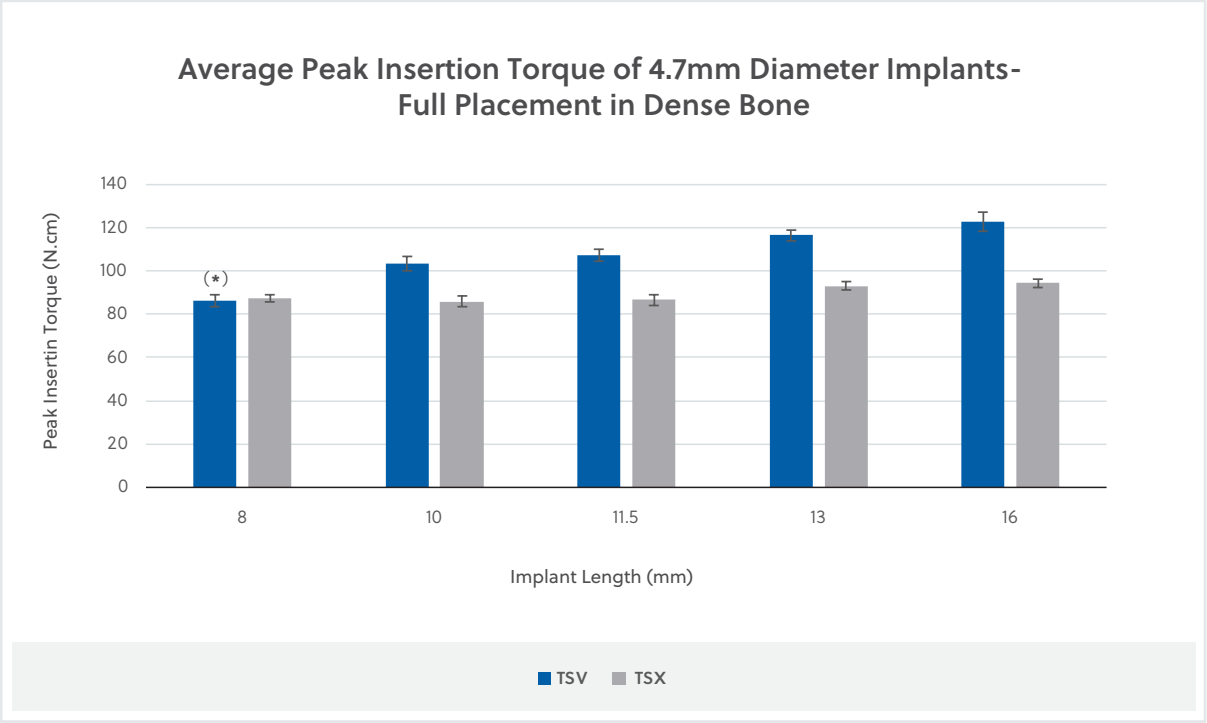

Fig. 10 *Peak insertion torque data measured for 4.7mm diameter TSV and TSX Implants placed following full placement protocol in dense bone at varying lengths of 8.0mm to 16mm.*

(*) There is no 3.1mm TSV, Data is from the 3.1mm Eztetic Implant.

The average peak insertion torque of TSX Implants was compared when placed following full placement protocol in dense and soft bones *(Figure 11)*. While the average peak insertion torque in dense bone was higher than in soft bone overall, the average peak insertion torque from the soft bone full placement protocol across all the diameters was always higher than 35 N.cm.

The difference between the data from dense and soft bone full placement protocol was minimal for 5.4 and 6mm implants, and indeed the values were approaching 80 N.cm when placed in soft bone, suggesting these implant diameters may be particularly suitable for placement in soft bone of the posterior maxilla.[1]

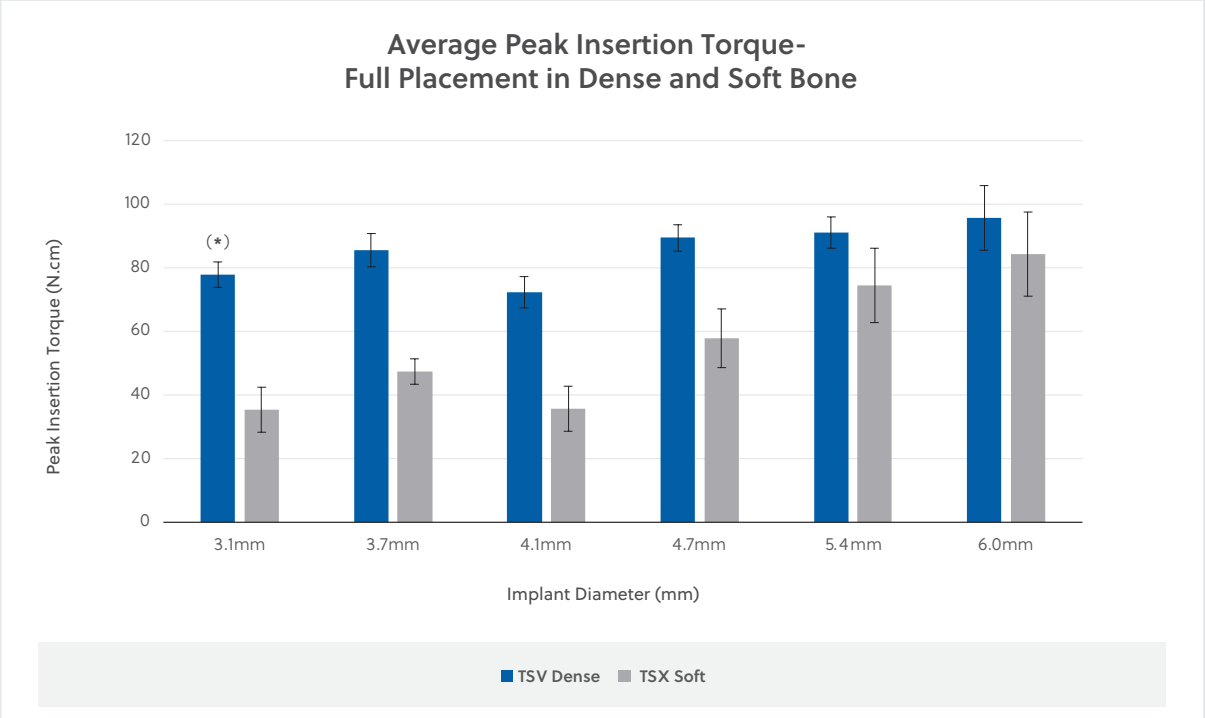

Fig. 11 *Peak insertion torque data measured for TSX Implants placed following full placement protocol in dense and soft bone with diameters varying from 3.1mm to 6mm at varying lengths of 8.0mm to 16mm. Data from different implant lengths have been averaged for a given diameter.*

(*) There is no 3.1mm TSV, Data is from the 3.1mm Eztetic Implant.

Full Placement Protocol: ISQ Data

The average ISQ for the TSX Implants placed following full insertion protocol in dense bone was ≥ 74 across all the tested diameters when averaged across all the tested lengths *(Figure 12)*.

There was no significant difference between ISQ of TSV and TSX Implants, and the data indicate a high stability of all the tested implants.

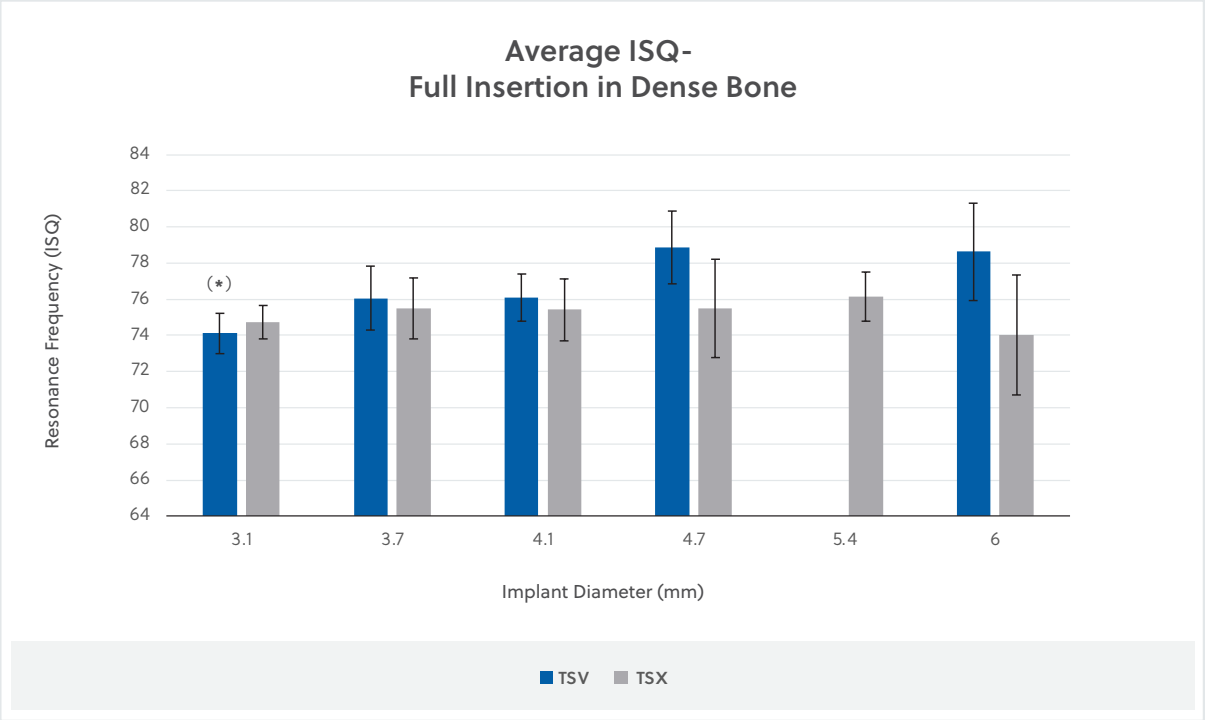

Fig. 12 *ISQ data measured for TSV and TSX Implants placed following full placement protocol in dense bone with diameters varying from 3.1mm to 6mm at varying lengths of 8.0mm to 16mm. Data from different implant lengths have been averaged for a given diameter.* ***NOTE:*** *The 5.4mm diameter does not exist in the TSV Implant line.*

(*) There is no 3.1mm TSV, Data is from the 3.1mm Eztetic Implant.

To examine the ISQ values at different implant lengths, 4.7mm diameter implants were chosen and the average ISQ data were measured across different implant lengths for the given diameter. Although the average ISQ was lower for the TSX Implants compared to TSV at all the tested lengths, the measured values were all above 70 *(Figure 13)*, indicating a high stability of all the tested implants.

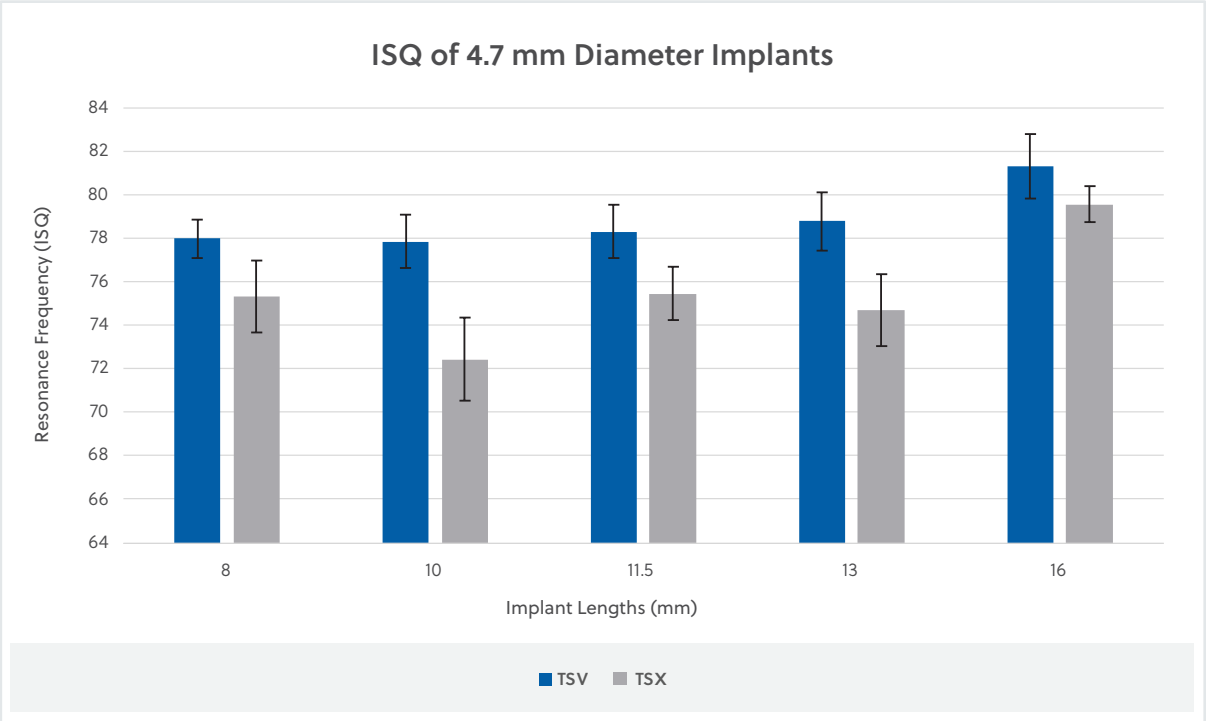

Fig. 13 *ISQ data measured for 4.7mm diameter TSV and TSX Implants placed following full placement protocol in dense bone at varying lengths of 8mm to 16mm.*

Full Placement Protocol: IBIC Data

The IBIC data were analyzed using box plots to show the data distribution across the implant diameters and lengths. The graphs were plotted inclusive median. The median marks the mid-point of the data and is shown by the line that divides the box into two parts. Half of the data are greater than or equal to this value and half are less. The outliers have been excluded. The middle box represents the middle 50% of data values (inter-quartile), which range from a lower to an upper quartile. Seventy-five percent of the data values fall below the upper quartile, and twenty-five percent fall below the lower quartile. The upper and lower whiskers represent scores outside the middle 50%.

A comparison of TSV and TSX percentage IBIC under full engagement across different diameters for a given length *(Figure 14a and c)* indicates an overall higher median IBIC% for TSX compared to TSV, except for 8mm length. Furthermore, more than 75% of measured IBIC% values for TSX fall above 30%, whereas for TSV of 11.5, 13, and 16mm lengths, the median is <=30%. For 8mm length, even though the median is slightly lower for TSX than TSV, higher IBIC% is measured for certain diameters, as shown by the upper whisker.

Percentage IBIC under full engagement across different lengths for a given diameter *(Figure 14b and 14d)* also indicates an overall higher median IBIC% for TSX compared to TSV, except for 3.1mm diameter. Furthermore, 100% of the measured IBIC% values for TSX fall above 30% regardless of diameter and length (except for 6mm), however, the variation is larger for TSV and the IBIC% values fall below 30% for 4.1, 4.7, and 6mm diameters.

Fig. 14c

Implant Length (mm)	TSV Median IBIC%	TSX Median IBIC%
8	43.8	40.6
10	34.7	36.4
11.5	30.2	34.6
13	27.1	34.5
16	24.1	34.6

Fig. 14a

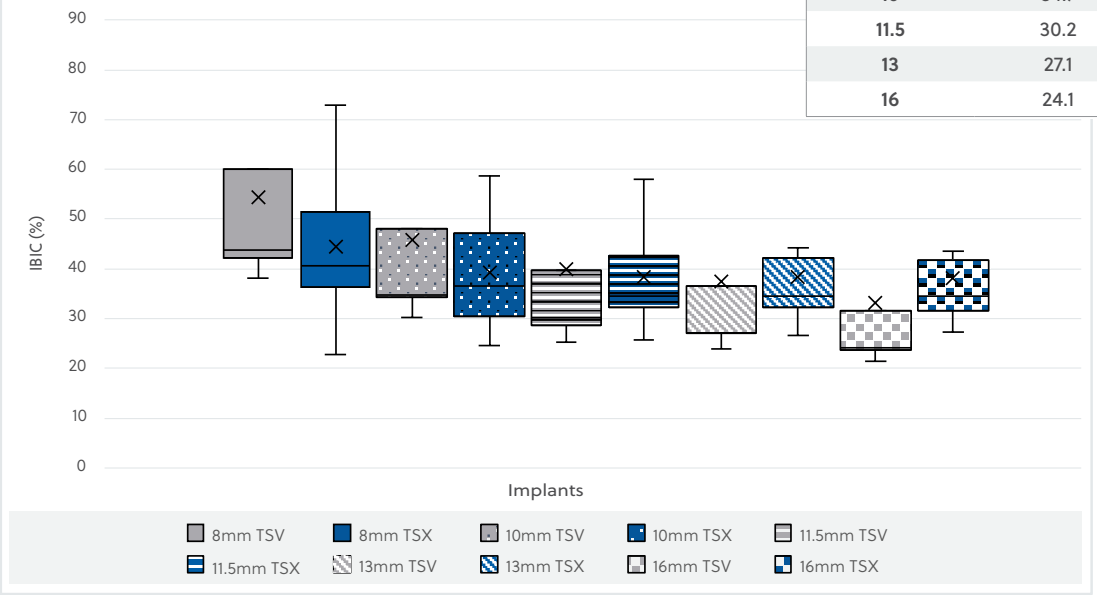

Fig. 14d

Implant Diameter (mm)	TSV Median IBIC%	TSX Median IBIC%
3.1	76.2	58
3.7	39.7	44.6
4.1	30.2	36.4
4.7	28.6	32.8
5.4	-	32
6.0	25.2	25.8

Fig. 14b

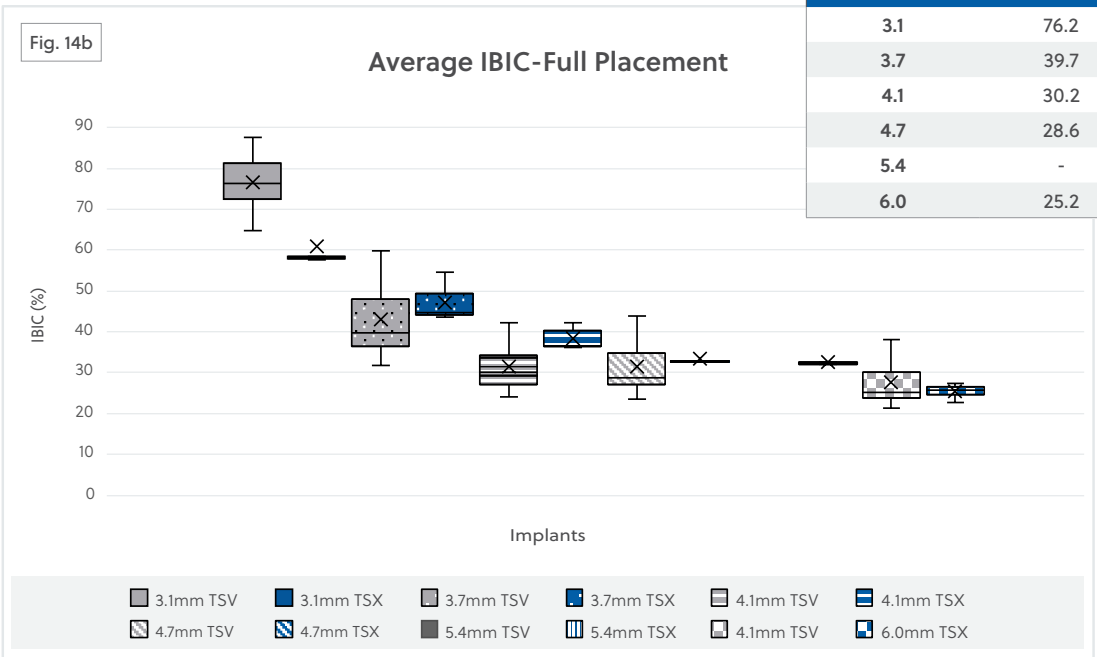

Fig. 14 *IBIC (%) data measured for TSV and TSX Implants placed following full placement protocol in dense bone with varying diameters of 3.1mm to 6mm at varying lengths of 8.0mm to 16mm. (a) Data from different implant diameters have been averaged for a given length. (b) Data from different implant lengths have been averaged for a given diameter. NOTE: The 5.4mm diameter does not exist in the TSV Implant line. The tables in (c) and (d) show median IBIC% of the TSV and TSX Implants in full placement across different lengths and diameters, respectively. NOTE: Half of the measured IBIC% fall above and half fall below the median values.*

Apical Placement Protocol: Insertion Torque Data

The average peak insertion torque of TSX Implants when apical placement protocol is followed is higher than the TSV Implants across different diameters for all the tested implant lengths *(Figure 15)*. This confirms that the design improvements of the TSX Implant have resulted in significant improvements in the apical stability of the implants, thus making it a better candidate to be placed in fresh extraction sockets.[1]

The insertion torque values are further increased when the apical extraction protocol is followed (i.e. the undersized osteotomy of apical placement).

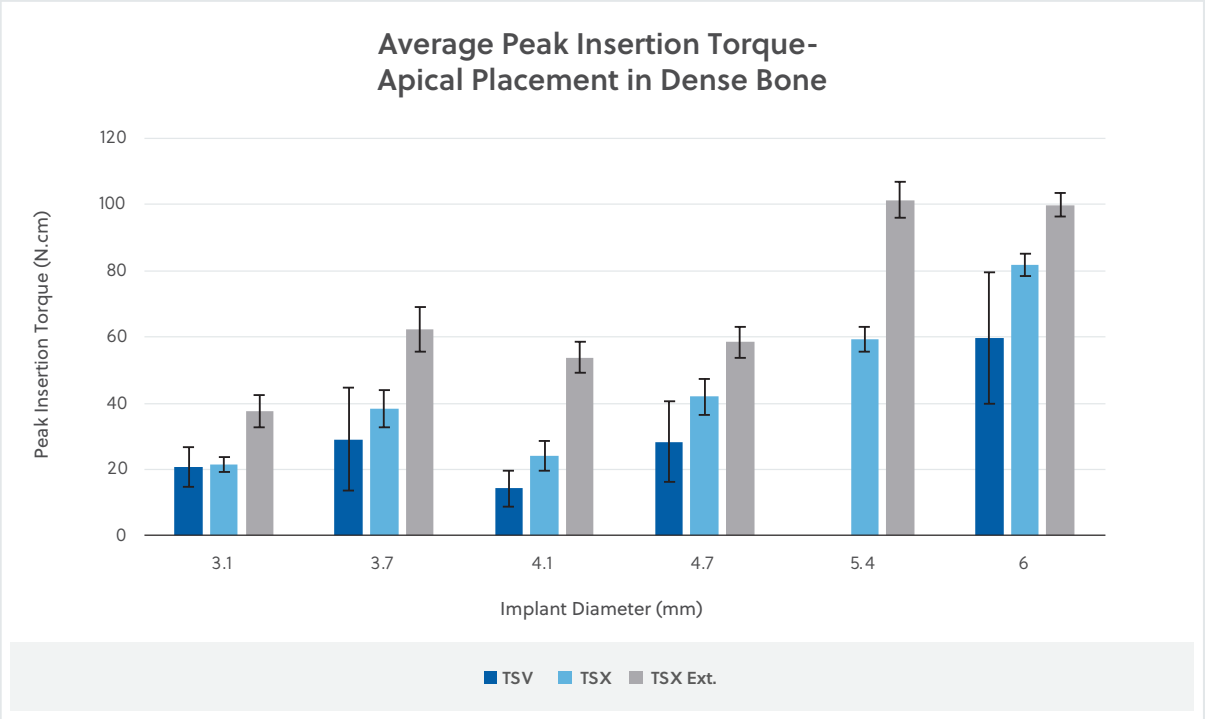

Fig. 15 *Peak insertion torque data measured for TSV and TSX Implants placed following apical placement protocol in dense bone with diameters varying from 3.1mm to 6.0mm at varying lengths of 8mm to 16mm. The peak insertion torque data of TSX (labeled TSX Ext.) Implants placed following apical extraction protocol are also presented. Data from different implant lengths have been averaged for a given diameter. NOTE: The 5.4mm diameter does not exist in the TSV Implant line.*

To take a more detailed look at the apical insertion torque data across different implant lengths for a given diameter, 4.7mm implant diameter at varying lengths of 8, 10, 11.5, 13, and 16mm was chosen *(Figure 16)*. The peak insertion torque data for TSX was considerably higher than TSV, except for 8mm where no differences were observed. The torque values are further noticeably increased when the apical extraction protocol is followed (i.e. the undersized osteotomy of apical placement) across all the tested lengths.

These findings again indicate the design improvements of the TSX Implant have resulted in significant improvements in the apical stability of the implants as compared to TSV.

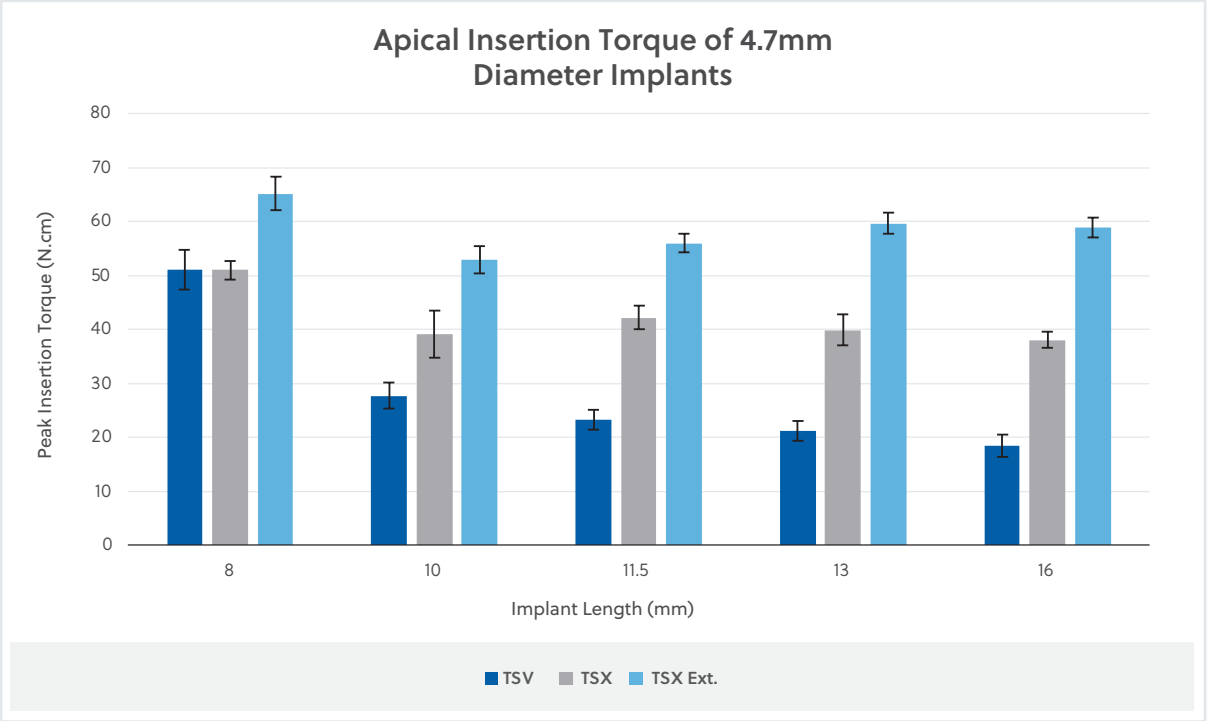

Fig. 16 *Peak insertion torque data measured for 4.7mm diameter TSV and TSX Implants placed following apical placement protocol in dense bone and at varying lengths of 8mm to 16mm. The peak insertion torque data of TSX Implants placed following apical extraction protocol (labeled as TSX Ext.) are also presented.*

Apical Placement Protocol: IBIC Data

Figures 17a and 17c present a comparison of TSV and TSX percentage IBIC under apical engagement across different diameters for a given length. They indicate an overall higher median IBIC% for TSX compared to TSV, except for 8mm length.

These differences are more noticeable than those measured in full placement *(i.e. Figure 14)*. 100% of measured IBIC% values for TSX fall above 30% regardless of implant diameter and length, whereas for TSV of 11.5, 13, and 16mm lengths, all fall below 30%.

Implant Length (mm)	TSV Median IBIC %	TSX Median IBIC %
8	41.4	34.6
10	27.5	32.7
11.5	20.3	32.1
13	20.2	32
16	18.1	32

Fig. 17c

Fig. 17a

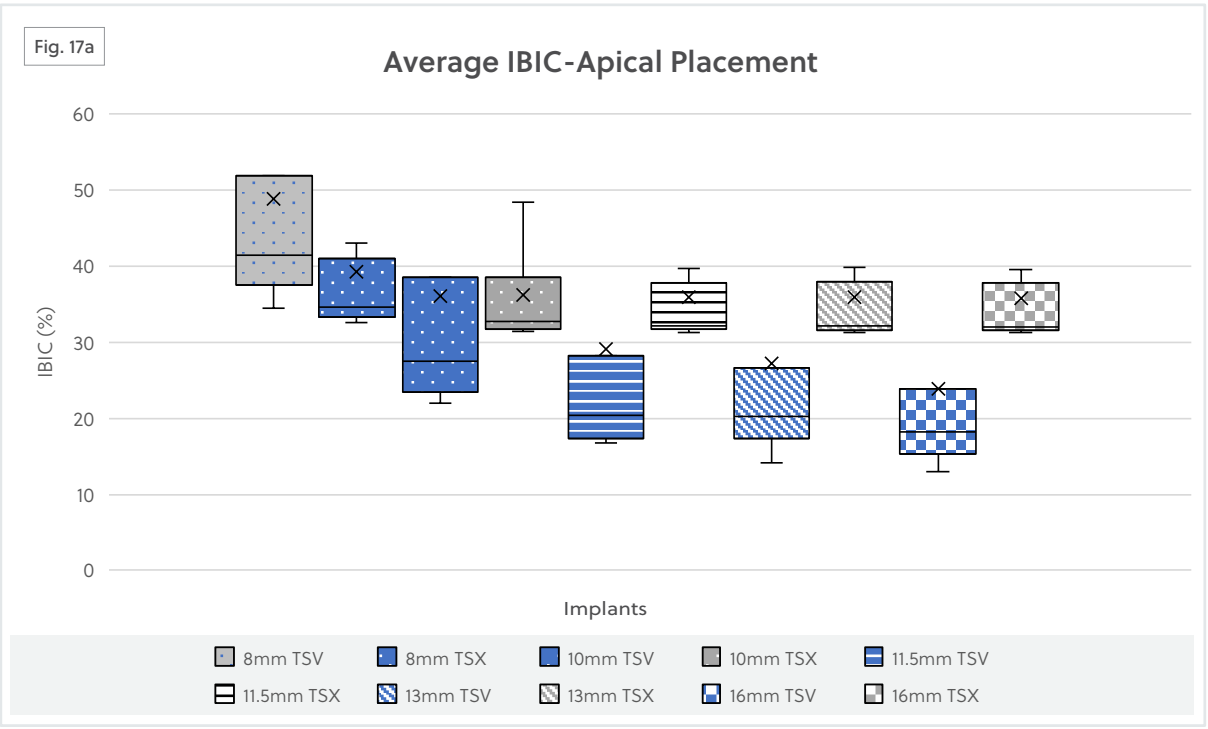

A comparison of TSV and TSX percentage IBIC under apical engagement across different lengths for a given diameter is provided in Figures 17b and 17d.

Figure 17b and 17d also confirm a considerably higher IBIC% for TSX compared to TSV, except for 3.1mm diameter. Similar to Figure 17a, 100% of IBIC% values for TSX fall above 30% regardless of implant diameter and length. However, the variation is larger for TSV, with some of the IBIC% values fall below 20% for 4.1, 4.7, and 6mm diameters.

Implant Diameter (mm)	TSV Median IBIC %	TSX Median IBIC %
3.1	62.5	48.4
3.7	28.2	40.2
4.1	16.7	32.4
4.7	20.3	31.6
5.4	–	31.3
6.0	17.2	31.7

Fig. 17d

Fig. 17b

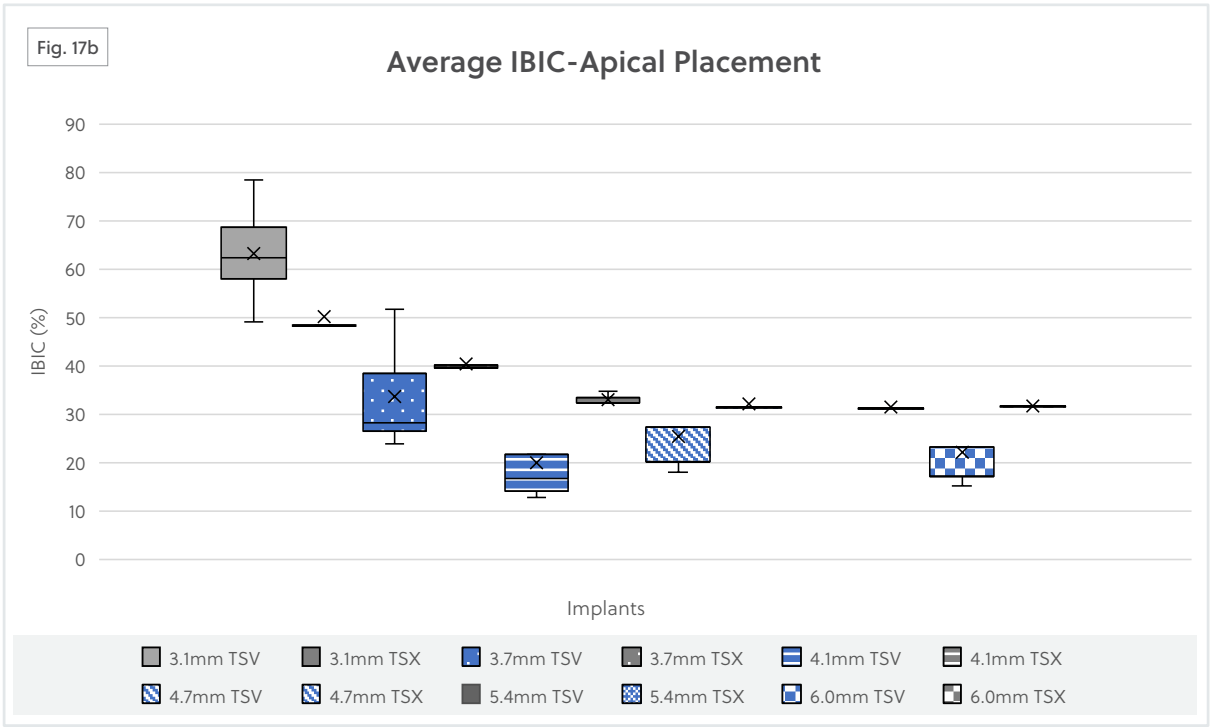

Fig. 17 *IBIC (%) data measured for TSV and TSX Implants placed following apical placement protocol in dense bone with varying diameters of 3.1mm to 6.0mm at varying lengths of 8mm to 16mm. (a) Data from different implant diameters have been averaged for a given length. (b) Data from different implant lengths have been averaged for a given diameter. NOTE: The 5.4mm diameter does not exist in the TSV Implant line. The tables in (c) and (d) show median IBIC% of the TSV and TSX Implants in apical placement across different lengths and diameters, respectively. NOTE: Half of the measured IBIC% fall above and half fall below the median values.*

Insertion Torque Profile

As observed with the insertion torque data above, extremely high insertion torque values of ~160 N.cm could be achieved following certain large diameter protocols with TSV Implants. However, the TSX Implant's new design successfully maintained the peak insertion torque values below a threshold of 100 N.cm when placed following both full and apical insertion protocols yet providing excellent primary stability due to increased IBIC. The torque profiles of both systems under full and apical placement conditions were reviewed, and noticeable differences were observed *(Figure 18)*.

The insertion torque profile of the TSV Implant shows a linear increase as the implant engages with the bone and reaches a peak value when the collar is fully seated; however, the insertion torque profile of the TSX Implant linearly increases in the beginning, and remains steady until it finally reaches a peak value once the implant is fully seated. The torque profiles of TSV and TSX Implants are similar when apical placement protocol is followed.

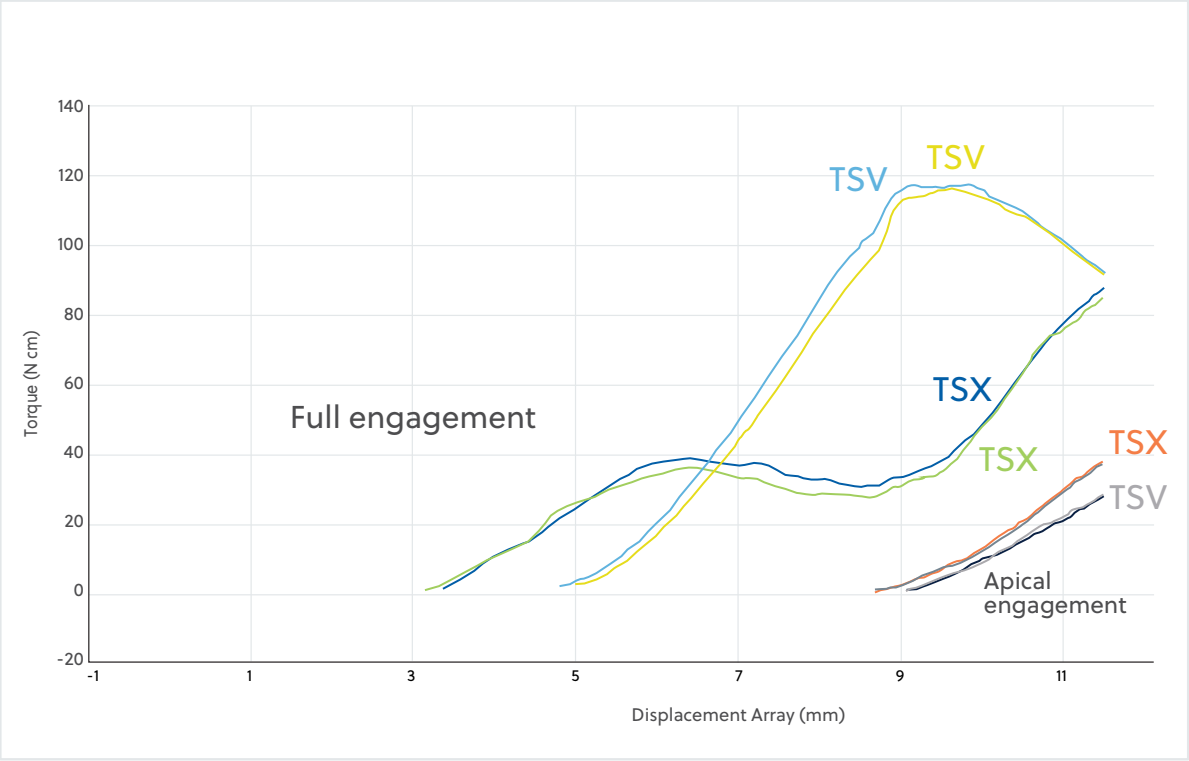

Fig. 18 *Torque profiles of 4.7mm x 11.5mm TSV and TSX Implants following full and apical placement protocols.*

SUMMARY

TSX Design for Primary Stability

The TSX Implant is indicated for immediate loading and immediate extraction placement when adequate primary stability and occlusal load are present. Full placement protocol data of the TSX Implant in dense bone shows that it achieves similarly high primary stability as TSV, as demonstrated by ISQ and insertion torque measurements greater than 70, via increased IBIC due to the deep cutting threads. TSX placement in soft bone also demonstrated high primary stability with the soft bone drilling protocol, with > 35 N.cm insertion torque and mean of 60 N.cm across all diameters.

The TSX Implant provides significantly more apical stability than TSV, and this stability can be further enhanced when following the new extraction protocol for immediate placement. While the TSX Implant has an aggressive cutting profile, the TSX Implant follows the drilled osteotomy and does not track off course from the intended placement.[1]

The New TSX Design for Peri-Implant Health

A variety of factors affect the long-term peri-implant health of dental implants. The TSX Implant design incorporates multiple features and concepts that may contribute to crestal bone maintenance and mitigate peri-implantitis risk, including platform switching, implant-abutment connection stability and strength, and a contemporary hybrid surface.[2-34]

Platform Switching

The new TSX Implant incorporates platform switching, a technique shown to maintain crestal bone levels, due to the newly designed coronally beveled seating area *(Table 1)*. Figure 19 shows the degree of platform switching (PLS) on TSV *(Figure 19a, c)* and TSX Implants *(Figure 19b, d)* of 4.7mm diameter and 13mm length when Encode® Emergence healing abutments and Hex-Lock® abutments were seated.

As evident from the yellow lines, which follow the contour of the implant-abutment junction, the PLS has increased in the new TSX Implant system compared to TSV. While the TSV Implant follows a platform match for 4.5mm collar diameter using a 4.5mm diameter Encode abutment, the TSX Implant accommodates a 3.5mm diameter Encode abutment on the 4.5mm collar diameter.

TSX/TSV Implant Diameter (mm)	TSX Platform Diameter (mm)	TSV/Eztetic Platform Diameter (mm)
3.1	2.9	2.9
3.7	3.5	3.5
4.1	3.5	3.5
4.7	3.5	4.5
5.4	4.5	N/A
6.0	4.5	5.7

Table 1: *PLS dimensions for TSX and TSV Implants of varying diameters.*

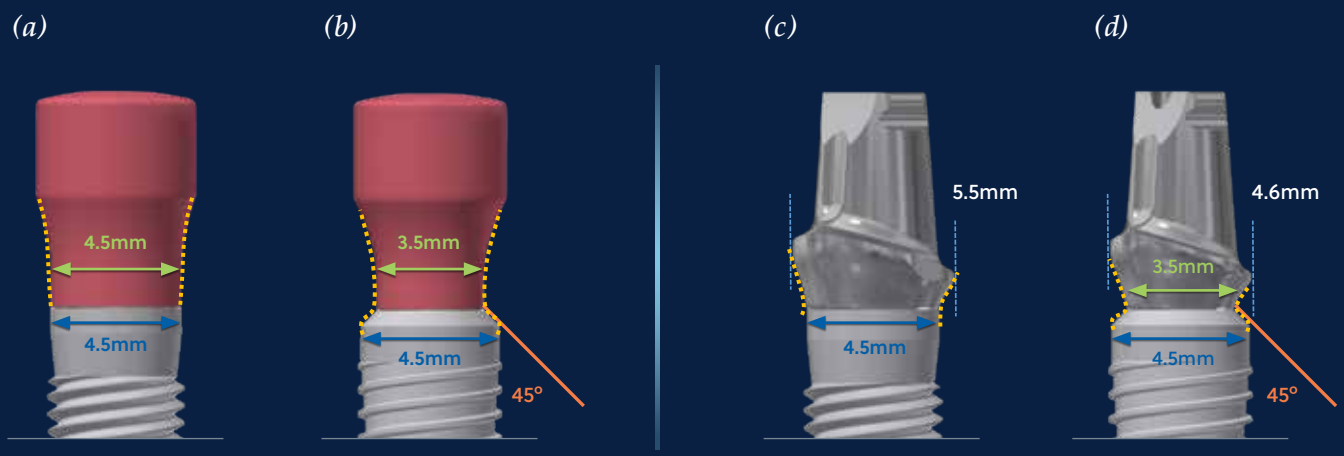

Fig. 19 *CAD models of (b,c) Encode Emergence healing abutment on (a) TSV and (b) TSX, and (c,d) Contour Hex-Lock Abutment on (c) TSV and (d) TSX. The yellow dashed lines were manually drawn to follow the contour of the implant-abutment junction to provide a visual reference of the space for soft tissue provided by the TSX platform switching design compared to TSV.*

Platform switching is a technique in which an abutment that is one size smaller than the implant platform is placed; thus it shifts the perimeter of the implant-abutment junction (IAJ) horizontally inward toward the central axis of the implant away from the outer edge of the implant platform.[39]

The reduced vertical crestal bone loss resulting from a platform switching was first noticed coincidently on the Implant Innovations, Inc. (3i, Palm Beach Gardens, FL, USA) wide-diameter implants of 5mm and 6mm, which were introduced in 1991 with restorative platforms of the same dimensions. However, there were no matching wide-diameter prosthetic components available at the time, and as a result, most of the initially placed implants were restored with standard 4.1mm diameter components creating a dimensional mismatch between the implant seating surface diameter and the diameter of the prosthetic component.

Upon reviewing radiographs after an initial 5-year period, the amount of crestal bone remodeling was noticeably reduced, with many platform switched restored implants exhibiting no vertical loss on crestal bone height.[39] Ever since, numerous reports have been published on the effect of platform switching on crestal bone level, all of which conclude that PLS is an effective approach to preserving crestal bone height.[2-14] Some of the recent examples are the two studies by Glibert, et al.[8] and Duque, et al.[9] using Osseotite Implants and one by Amato et al.[10] using T3® Implants. The outcomes of these studies provided direct comparisons between the absence and presence of PLS in the same implant design. Cumulative survival rates did not appear to be impacted by the presence or absence of PLS; however, statistically significant reductions in the marginal bone loss were observed for the implants with PLS.

Connection Stability

The implant–abutment interface geometry seems to be an influencing factor for stress and strain transmission around the implant. It has been shown that the peak bone stresses resulting from vertical load components and those resulting from horizontal load components arise at the top of the marginal bone and coincide spatially. These peak stresses added together produce a risk of stress-induced bone resorption.[20] Therefore, to reduce crestal bone loss, the fit between the implant and abutment and the connection stability should be enhanced.

The TSX Implant follows the same proprietary internal hexagon-and-thread connection of the TSV Implants featuring a variety of friction-fit restorative components that serve implant diameters ranging from 3.7mm to 6.0mm. The friction-fit internal hex connection features a lead-in bevel that acts as a conical seating surface to reduce horizontal stresses at the bone-implant interface and maintain crestal bone level, followed by a 1.5 mm-deep hexagonal hole and an internal thread chamber below the hexagon *(Figure 20)*.

The friction-fit internal connection is machined to provide a slip-fit in the conical portion of the coupling and a 1° of taper in the hex portion to provide a friction-fit connection with the implant, which forms a virtual cold weld and reduces abutment micro-movements and screw loosening when tightened to the recommended 30 N.cm of applied torque.[15] The intimate locking connection between the implant and abutment thus eliminates rotational micromovement and tipping.[15] The friction-fit connection has also been documented to eliminate the effect of occlusal vibration and distributes forces deeper within the implant than a standard external hexagon connection, which shields the abutment screw from excessive loading.[40] Lateral forces are transmitted directly to the walls of the implant and the mated implant-abutment bevels, which provides greater resistance to interface opening than a butt-joint connection.[40]

The 3.1mm TSX Implant employs the double friction-fit conical internal hex connection developed for narrow anterior tooth replacement with the introduction of the 3.1mm Eztetic Implant in 2015. The 3.1mmD Eztetic Implant features a 2.9mmD prosthetic platform. A 1.3mm deep, 17° internal cone extends from the outer-most diameter (2.9mmD) of the implant platform to the internal hex of the implant. The internal hex is 2.1mm flat-to-flat with a depth of 1.7mm *(Figure 20)*. The 3.0 mm deep conical connection is designed to distribute stresses deep into the implant and away from the crestal bone to aid in crestal bone maintenance.[1]

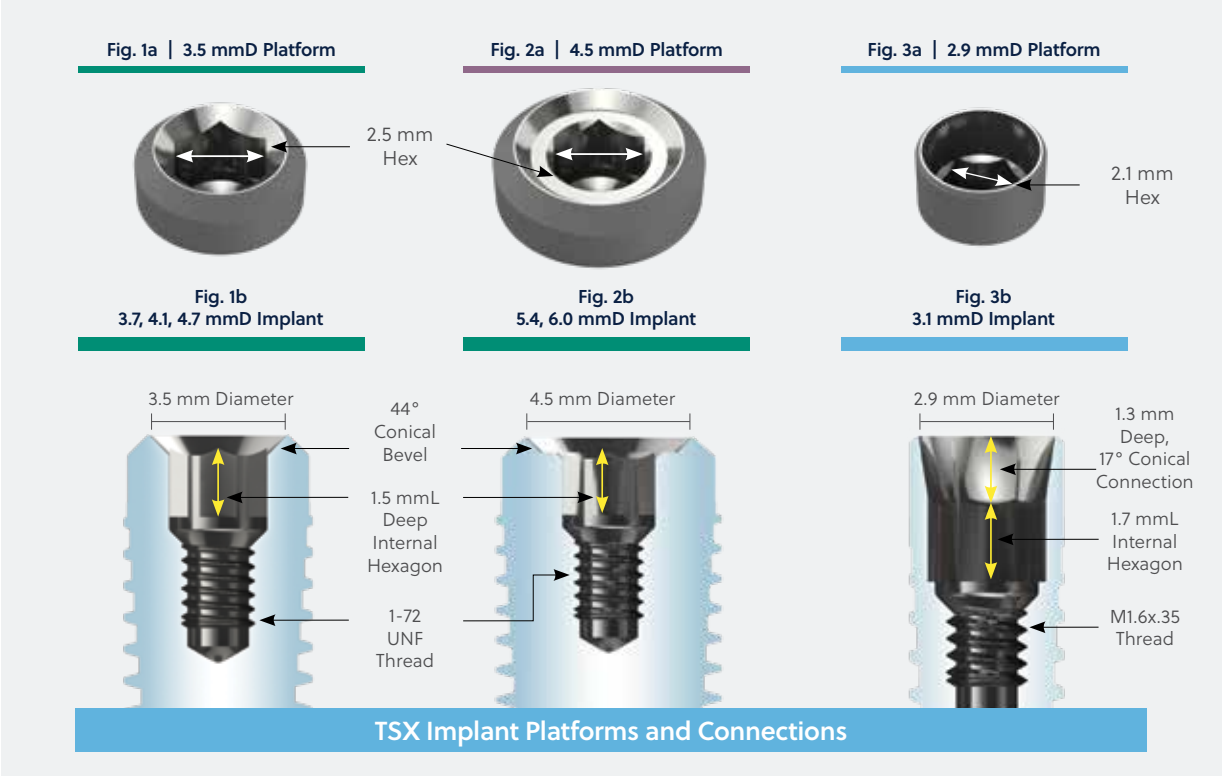

Fig. 20 *(Figures 1a, 1b, 2a and 2b) show internal hex connection of TSX Implants in 3.7mm to 6.0mmD. (Figures 3a and 3b) show conical hex connection of 3.1mmD TSX Implant.*

Connection Strength

The TSX connection has been further strengthened by increasing the wall thickness coronally *(Figure 21 and Table 2)* to avoid possible breakage and opening up of the coronal portion. The wall thickness increase of 11.5mm length TSV and TSX Implants of varying diameters are shown in *Table 2.* As evident from the percentage increase, significant improvements have been made across different diameters to the TSX wall thickness, specifically for 3.7, 4.1, and 6mm diameters.

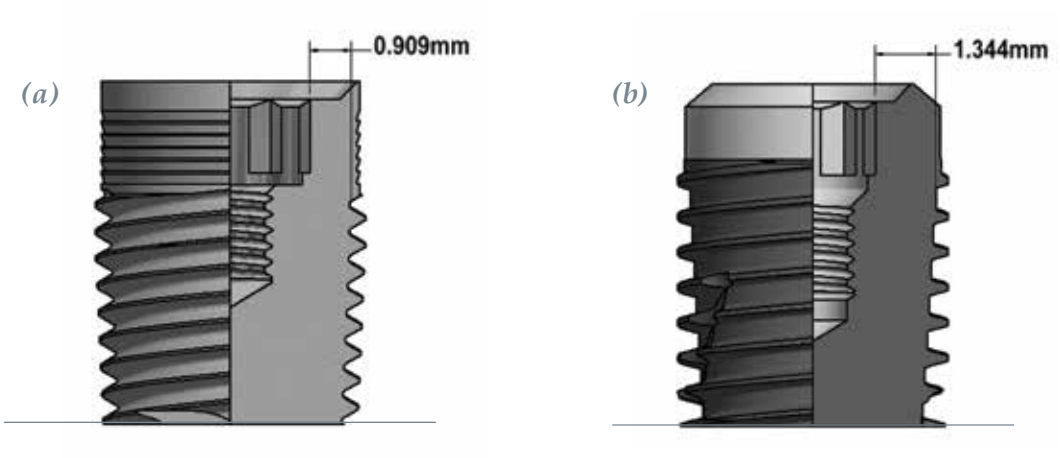

Fig. 21 *Wall thickness of a 6mm x 11.5mm (a) TSV and (b) TSX Implant in the coronal portion of the internal connection.*

Diameter (mm) X Length (mm)	Wall Thickness (mm)		Percentage Increase
	TSV	TSX	
3.1 x 11.5	0.180	0.231	28%
3.7 x 11.5	0.095	0.277	186%
4.1 x 11.5	0.274	0.541	97%
4.7 x 11.5	0.592	0.775	31%
5.4 x 11.5	N/A	1.17	N/A
6.0 x 11.5	0.909	1.344	48%

Table 2: *Wall thickness of 3.1, 3.7, 4.1, 4.7, and 6mm diameter and 11.5mm length TSV and TSX Implants.*
NOTE: The 5.4mm diameter does not exist in the TSV Implant line.

To assess the impact of increased wall thickness of TSX Implant compared to traditional TSV Implant, cyclic fatigue testing was conducted on both systems based on the ISO 14801 method. TSX and TSV Implants (3.7mm diameter and 13mm length) were potted in phenolic resin powder and hot mounted under temperature/pressure specification in accordance with ISO14801:2016 (Dentistry – Implants – Dynamic fatigue test for endosseous dental implants) and FDA class II Special Controlled Guidance Document for Root-form Endosseous Dental Implants.

To mimic the worst-case scenario, 3mm bone resorption was simulated by supporting the implants 3mm below the anticipated crestal bone level. Furthermore, 30° abutment angulation with implant long axis at 40° was chosen, leaving 10° of uncorrected angulation. Abutment screw torque was set at 30 N.cm prior to testing. A total of 5 samples per group were used to determine the mean static failure load and a total of 12 samples per group were tested under cyclic fatigue testing. Maximum endurance limit at which at least three samples reached 5 x 10^6 cycles of loading at 15 hz in air was then determined. Following the completion of 5 x 10^6 cycles, each implant/abutment was inspected for damage per ISO 14801: 2016.

Maximum endurance limit was measured 283 N.cm for TSX and 234 N.cm for TSV, corresponding to 21% increase in fatigue strength for the TSX Implant compared to TSV Implant. This is attributed to the increased wall thickness of the TSX Implant compared to the TSV Implant.

Coronal Surface

The TSX Implant is designed with a contemporary hybrid surface, meaning the implant collar *(Figure 22a-1)* and body *(Figure 22a-2)* present different surface morphologies and roughness. The implant collar (about 1.5mm coronal area) is dual acid-etched and represents Osseotite surface of the Osseotite alloy implant systems. The acid etching pits measure about ~ 1 - 3µm in diameter *(orange arrows on Figure 22b)*, and the surface roughness Sa value as measured by Keyence microscope is reported ~ 0.3 - 0.4µm.

The implant body has the MTX surface created by grit blasting the surface using hydroxyapatite particles as the blasting media. The surface features valleys and plateaus typical of a grit blasted surface *(Figure 22c)*, and the surface roughness Sa value measured by Keyence microscope is reported ~ 0.6 - 0.9µm.

The external-hexed Osseotite Implant was launched in 1996 with the dual acid-etched surface. The surface has now over two decades of clinical use and proven success documented in numerous global multi-center clinical studies[21-27] and meta-analyses.[28, 29] Clinical studies on Osseotite surface continue to demonstrate the benefits of increased contact osteogenesis, especially in poor-quality bone,[25] increased bone-to-implant contact,[30] and improved crestal bone maintenance[31] compared to machined surfaces.

The coronal part of an implant plays an important role not only in the osseointegration process but also in peri-implant tissue health. Different surface technologies have been developed to increase the surface roughness of dental implants to improve bone-to-implant contact and enhance the osseointegration process. Roughened implant collar surfaces have been suggested to maintain crestal bone height. Crestal bone loss around rough-surfaced (SLA) microthreaded neck implants has been shown to be significantly lower than smooth-surfaced neck implants.[41] The outcomes of a meta-analysis have also demonstrated that peri-implant bone loss around minimally rough implant systems was statistically less compared to the moderately rough and rough implant systems.[42]

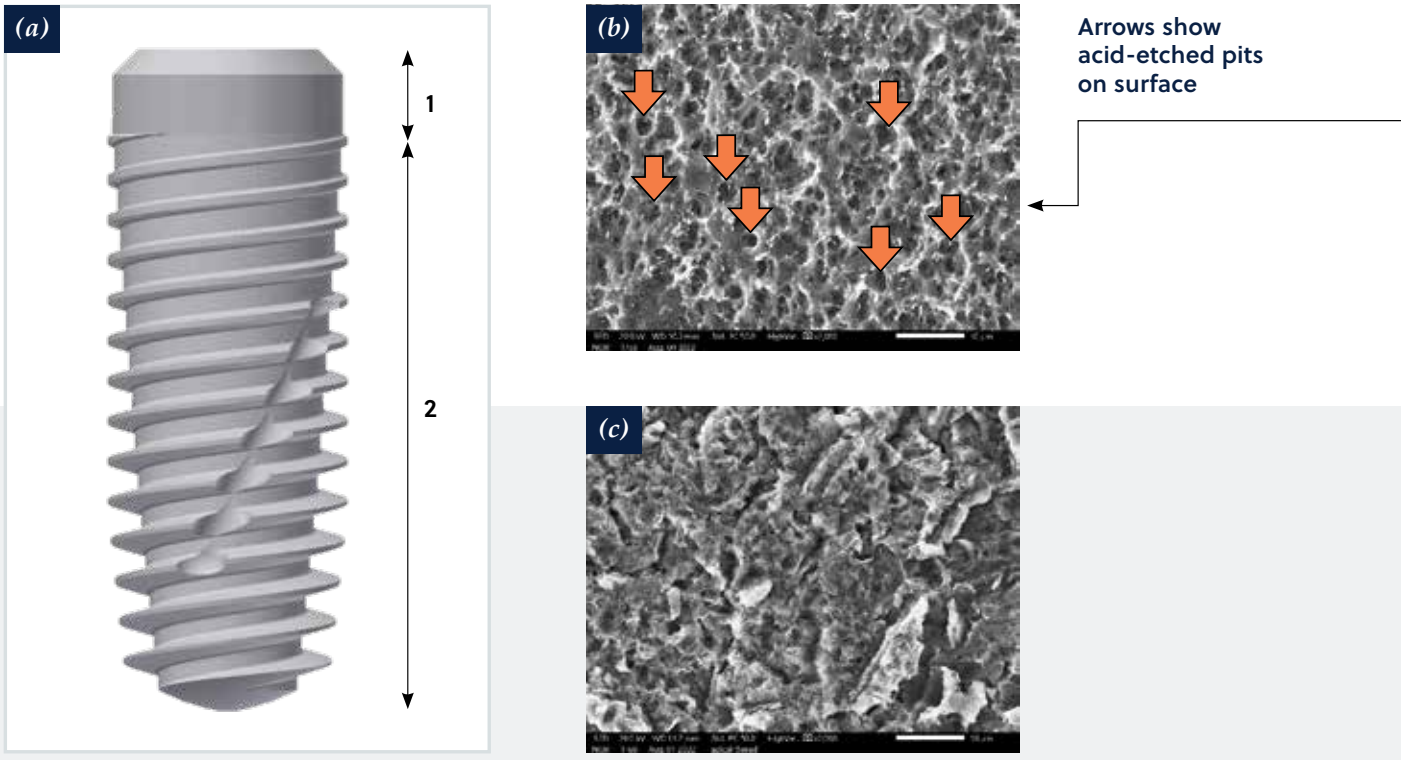

Fig. 22

(a) CAD model of the TSX Implant. (1) Implant collar and (2) Implant body.

(b) SEM micrograph of the surface in region 1, which is dual acid-etched and clearly shows acid etching pits (shown by orange arrows) measured ~ 1 - 3µm.

(c) SEM micrograph of the surface in region 2, which is grit blasted using hydroxyapatite as blasting media.

Furthermore, in a retrospective study that examined long-term crestal bone level changes around three implant systems with similar macrodesign but different micro-surface topography in a homogeneous patient population, mean crestal bone loss was significantly higher in the anodized implant group (TiUnite, Nobel) when compared to the hybrid implant (Osseotite, ZimVie) or the turned implant group.[43]

Finally, the loss of crestal bone was shown to be significantly less for the implants with acid etched collar (Osseotite) compared to the machined collar surface implants.[31]

During the peri-implant tissue healing process, there is a competition between the native tissues inclined to grow onto the implant surface versus the microbial microorganisms that seek to colonize and eventually form biofilm on the surface.[44, 45] The loss of soft tissue seal and alveolar bone would expose the collar, and in more severe cases, the body of the implant to the alveolar environment, and within about 30 minutes post-implantation, the microbiota can be identified on the surface.[46]

The surfaces with increased roughness that were initially designed for better osseointegration can now stimulate bacterial adhesion. In fact, sufficient evidence exists that the surface morphology and its roughness is one of the major contributing factors to the prevalence of peri-implantitis. It is believed that a reduced bacterial adhesion on implant surfaces might be clinically associated with a reduced risk or incidence of peri-implant infections.[47] A balance between osseointegration on the one hand and the absence of plaque accumulation on the other hand is necessary for successful implantation.

Therefore, on the TSX Implant, a surface finish was chosen for the implant coronal region based on the evidence on the morphology and degree of roughness that can maintain a reasonable balance between enhanced osteoconduction to implant collar and reduced bacterial adhesion to mitigate the risk of biofilm formation.

TSX Bacterial Adhesion Test Methods and Results

A preliminary bacterial culture study was conducted using cp-Ti implants with a dual acid-etched collar, demonstrating that the acid-etched collar may serve as a good coronal surface with desirable morphology and roughness to prevent increased bacterial adhesion associated with rougher surface textures compared to a smooth machined collar.[34] The TSX Implant is made of titanium alloy (Ti6Al4V). Therefore, another in vitro assay was conducted not only to test the adhesion of bacteria to a dual acid-etched surface on Ti alloy implants and compare that to cp-Ti counterparts, but also to employ a more clinically relevant strain of bacteria that can be found in peri-implantitis cases. For ease of establishing the protocol, this assay was conducted using Ti discs representing the implant surfaces.

Bacterial Adhesion Testing – CP4 Titanium / Titanium Alloy Comparison

CP4 Titanium / Titanium Alloy Comparison Testing Methods

Tested Surfaces	This experiment was designed using five groups of samples (discs of 14.5mm diameter and 2mm height). Three groups of discs were made of Ti6Al4V with machined (Machined Alloy), dual acid-etched (Osseotite Alloy – representing TSX Implant collar surface), and grit-blasted surfaces (MTX – representing TSX Implant body surface). The other two groups were made of grade 4 cp-Ti with machined (Machined CP4) and dual acid-etched (Osseotite CP4) surfaces. The latter two groups were chosen to examine the effect of material type (CP4 vs. Ti6Al4V) on the adhesion of bacteria. All the samples were processed, post-cleaned, and sterilized identical to commercial implant post-processing to ensure the final surface possesses had the same surface properties as the final implants.
Surface Characterizations	The surface morphology of the discs was examined with a scanning electron microscope (SEM – JEOL Model JSM-IT500HR). All the disc surfaces were mapped with a Keyence microscope (VK-X1050), and the surface roughness of each sample was calculated and analyzed with MultiFile Analyzer (Keyence). The Sa value, i.e., the arithmetical mean height of the assessed area, was used to measure surface roughness.
Bacteria Type	The chosen strain of pathogenic bacteria was Streptococcus Oralis (S. Oralis) (ATCC 6249), which was purchased from ATCC and cultured in brain heart infusion (BHI) broth (RemelTM). The reason to choose this specific strain of bacteria is that it is the predominant initial colonizer found at infected oral implant sites, attaches to the salivary pellicle, and establishes a kind of anchor for further attachment of intermediate and late pathogenic colonizers, thus can enhance bacterial pathogenicity.
Bacterial Culture	The sterilized discs were placed in 24 wells tissue culture plates, and 1mL of 10^5 CFU/ml of S. Oralis BHI suspension was added to each well. The plate was placed on a shaker at 100rpm and cultured at 37 °C for 7 hours. After the incubation period, all the samples were taken and washed with 1 X PBS (phosphate buffer saline) once. A Microbial Viability Assay kit-WST (Dojindo) was used to quantify the adhesion of S. Oralis on the discs. Briefly, the discs with adhered bacteria were placed in individual wells of a 24-well tissue culture plate, 300μL of WST solution was added to each well, and the culture was continued for 1 hour until the solution changed color. A 96-well plate was then used to transfer 100μL of the test solution from each sample, and the absorbance at 450nm was recorded with a plate reader (n=4 per group).
Bacteria Imaging	Fluorescent microscopy (Olympus microscope) was performed to visualize live and dead bacteria on the discs. For this, the staining was done with a LIVE/DEAD™ BacLight™ Bacterial Viability Kit by placing the discs with the adhered bacteria in 300μL of staining solution in a 24-well tissue culture plate and culturing at room temperature in the dark for 15 minutes. The live bacteria were stained green, and the dead bacteria, which must have stained red, were washed away during the washing steps and are not shown in the images. After getting fixed, dehydrated, and gold sputter coated, the bacteria adhered on the discs were also visualized using SEM (JEOL Model JSM-IT500HR).

Bacterial Adhesion Testing – CP4 Titanium / Titanium Alloy Comparison

CP4 Titanium / Titanium Alloy Comparison Testing Results and Discussion

Surface Roughness: The Sa values of the surfaces are shown in Figure 23a. The Sa value of machined CP4 (0.14µm) is lower than that of machined alloy (0.24µm). The reason is that the machining lines are more pronounced on the alloy discs because of their higher hardness compared to CP4 Titanium. The Sa value of Osseotite alloy (0.37µm) was lower than Osseotite CP4 (0.61µm). This is because the alloy material does not etch as easily as a CP4 surface due to its higher hardness. Finally, the Sa value of MTX is measured at around 1.27µm.

Fig. 23a

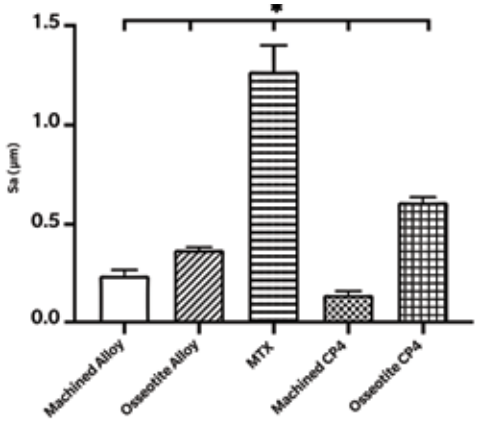

Fig. 23b

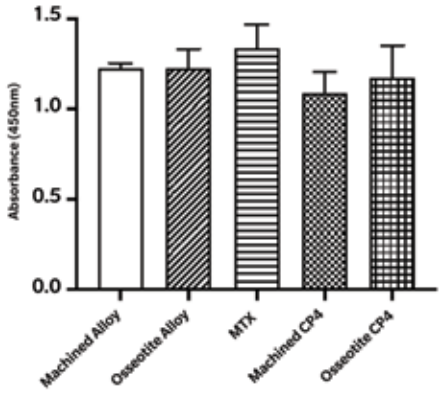

Fig. 23 *(a) Sa values of different surfaces. (b) Quantification of adherent live bacteria to the surfaces as measured by absorbance at 450nm. NOTE: The alloy is Ti6Al4V, and CP4 is commercially pure grade 4 titanium.*

Bacterial Adhesion: The number of live bacteria adhered to the surfaces was quantified by measuring the absorbance at 450nm. As shown in Figure 23b, there are no significant differences in the number of attached bacteria among the surfaces. Machined CP4 shows a slightly less number of adhered bacteria than machined alloy, which can be attributed to the lower Sa of the former compared to the latter. Both Osseotite CP4 and alloy showed a relatively similar number of adhered bacteria, even though Osseotite alloy has a lower Sa than Osseotite CP4. It is noteworthy that the amount of adhered bacteria on both are at the level of machined surfaces, even though their roughness is higher. Slightly more bacterial adhesion was observed on the MTX compared to machined and Osseotite alloy surfaces. These non-significant changes in the number of adhered bacteria on the surfaces that have significantly different Sa values confirm a cut-off roughness level around 1µm below which no significant differences are seen in the amount of adhered bacteria.

The fluorescent images showed the distribution of live bacteria (green color) on different disc surfaces *(Figure 24)*. A similar number of adhered bacteria was observed on both machined CP4 and Osseotite CP4, and on machined alloy and Osseotite alloy. However, overall, there seem to be fewer bacteria on CP4 surfaces compared to their alloy counterparts, but not statistically significant. Finally, MTX exhibited more adhered bacteria than Osseotite and machined surfaces.

Fluorescent Images (Taken at x10)

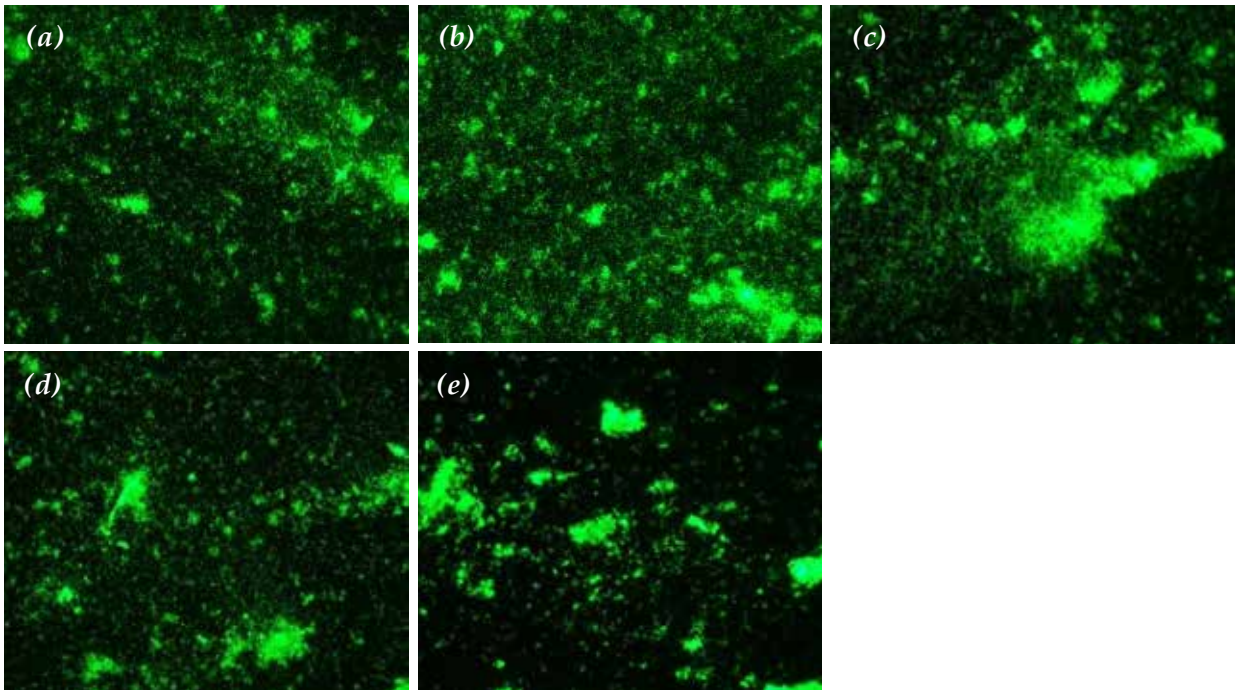

Fig. 24 *Fluorescent images of adherent live bacteria on (a) machined alloy, (b) Osseotite alloy, (c) MTX, (d) machined CP4, and (e) Osseotite CP4 disc surfaces following 7 hour incubation period.*

To investigate the attachment of the bacteria to the underlying surface textures, SEM images were taken, and the bacteria were color-coded for ease of visualization *(Figure 25)*. The findings were in line with the fluorescent images regarding the number of adhered bacteria on the surfaces. In terms of the pattern of adhesion, there seem to be differences between the textured vs. machined surfaces.

While the bacteria are lining up and forming chains on the machined surfaces, those on the textured surfaces have adhered more in a random fashion. Most bacteria groups are seen on the sharp edges of acid etching pits on Osseotite surfaces and the large micron grit blasting peaks of MTX.

SEM Images

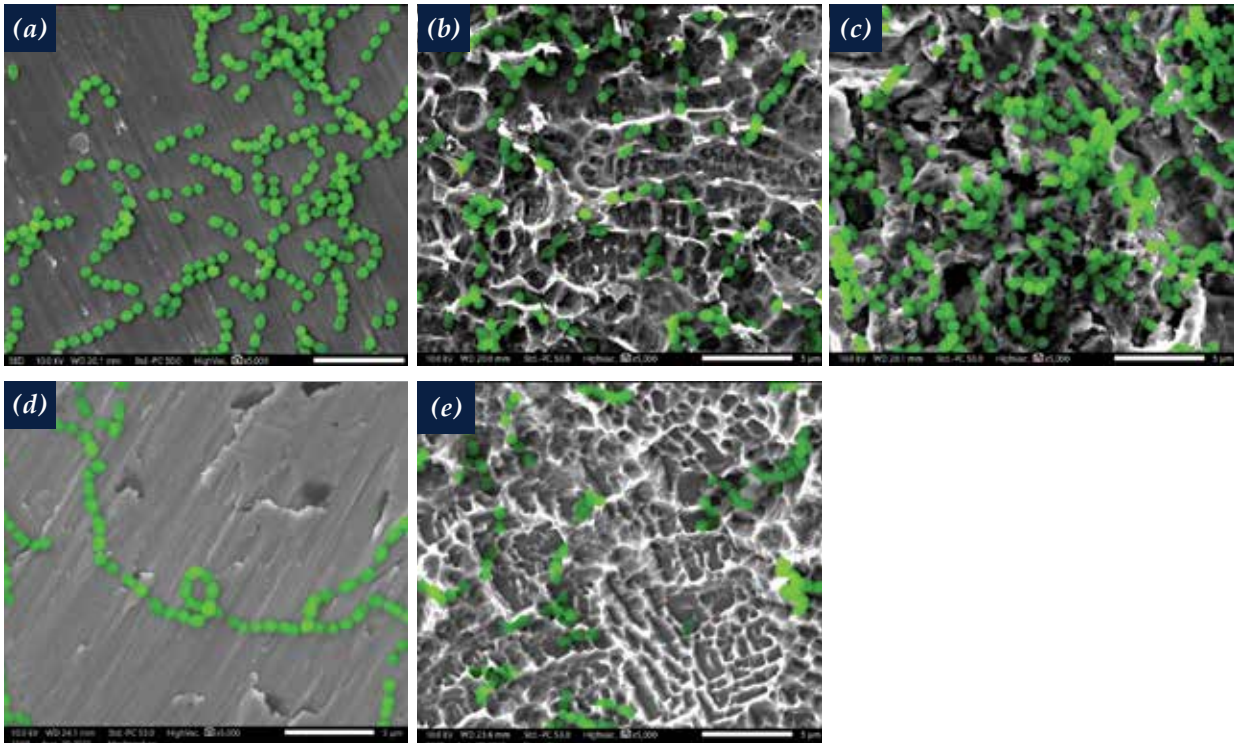

Fig. 25 *SEM images of adherent bacteria on (a) machined alloy, (b) Osseotite alloy, (c) MTX, (d) machined CP4, and (e) Osseotite CP4 disc surfaces following 7 hour incubation period. Attached bacteria were color coded in green using MountainsMap SEM Topo software (Digital Surf) for visualization purposes. Scale bars = 5µm.*

CP4 Titanium / Titanium Alloy Comparison Conclusion

The results of this in vitro assay showed that by applying dual acid etching on the collar of the TSX Implant, the amount of adhered bacteria is reduced compared to the traditional MTX surface but not increased compared to the machined surface. It was also confirmed that there are no significant differences between a dual acid-etched surface on the alloy compared to the CP4 titanium surface, which enables us to leverage the outcomes of the studies that have examined peri-implant health on CP4 Osseotite implants.

Bacterial Adhesion Testing – Competitive Comparison Study

The bacterial culture experiments were repeated using implants instead of discs to compare the adhesion of S. Oralis to the collar surface of the TSX Implant as compared to a series of other competitive implants made of both Ti alloy and CP4 Ti.

Competitive Comparison Testing Methods

Tested Surfaces	This experiment was designed using ten groups of implants *(Table 3)*. All the implants were purchased from their manufacturers and removed from their original packaging in the biological safety hood to avoid contaminations from the air before bacterial culture.

Implant Manufacturer	Implant Size	Surface Technology on Implant Collar	Method Surface Created	Implant Material
Nobel Biocare	4.3 mm x 13 mm	TiUltra	Anodization	Ti CP4
ZimVie	4.1 mm x 13 mm	Machined	Machining	Ti Alloy
ZimVie	4.1 mm x 13 mm	Osseotite	Dual acid etching	Ti Alloy
ZimVie	4.1 mm x 13 mm	MTX	Grit blasting	Ti Alloy
Implant Direct	4.2 mm x 13 mm	SBM	Grit blasting	Ti Alloy
Dentsply Sirona Astra Tech	4.2 mm x 13 mm	Osseospeed	Grit blasted (TiO blasted) Flouoride-modified	Ti CP4
Nobel Biocare	4.3 mm x 13 mm	TiUnite	Anodization	Ti CP4
MiS	4.2 mm x 13 mm	C1	Sand blasted and etched	Ti Alloy
Straumann	4.1 mm x 13 mm	SLA	Large-grit sand blasted and acid etched	Roxolid (Zr Ti alloy)
BioHorizons	4.2 mm x 13 mm	Laser-Lok	Laser machined	Ti Alloy

Table 3: *Ten groups of implants tested.*

Competitive Comparison Testing Methods

Surface Characterizations	The surface morphology of the implant collars was observed with a scanning electron microscope (SEM, JEOL Model JSM-IT500HR). All the collar surfaces were mapped with a Keyence microscope (VK-X1050), and roughness Sa values were analyzed with MultiFile Analyzer (Keyence). A total of 4 areas (144μm x 108μm) on each implant collar were measured.
Bacteria Type	The chosen strain of pathogenic bacteria was Streptococcus Oralis (S. Oralis) (ATCC 6249), which was purchased from ATCC and cultured in brain heart infusion (BHI) broth (RemelTM).
Bacterial Adhesion	All the implants were removed from their original sterile packaging in the biological safety hood, assembled onto a customized sterilized titanium fixture, and placed in a well of a 24-well tissue culture plate *(Figure 26)*. One ml of 106 CFU/ml of S. Oralis suspension was added to each well, and the plate was placed on a shaker at 100rpm and cultured at 37 °C for 4 hours. Each implant was then disassembled from the fixture and gently washed with 2ml of 1 X PBS once. A Microbial Viability Assay kit-WST (Dojindo) was used to quantify the adhesion of S. Oralis on the implant collar. Briefly, 300μL of WST working solution was added to each well of 24-well tissue culture plate, and the implants with adherent bacteria were placed upside down in each well, with only the implant collar submerging in the measuring solution, and incubated at 37° C for an hour. 100μL of the test solution from each well was then transferred to a 96-well plate and the absorbance at 450nm was measured with a plate reader (Synergy multi-mode reader, BioTek Instruments) (n=3 per group). The absorbance value indirectly reflects the number of adherent live bacteria.
Statistical Analysis	One-way ANOVA with Dunnett's multiple comparisons test was performed to determine the statistical differences between the groups (GraphPad Prism 8). The $p<0.05$ was considered significant.

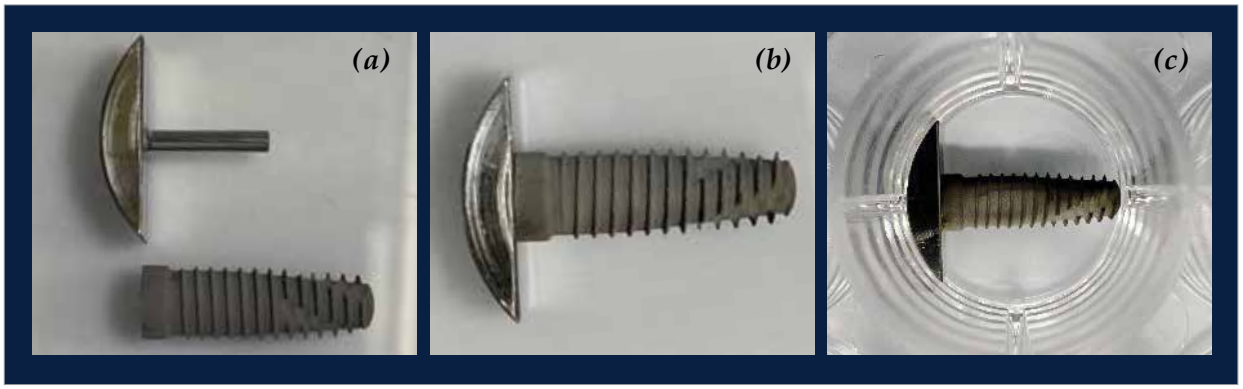

Fig. 26 *(a) Customized titanium fixture for mounting the implants. (b) Implant mounted on the fixture. (c) The fixture with the implant is placed in a 24-well plate for bacterial adhesion experiments.*

Bacteria Imaging	The adherent bacteria on the implant collar were further visualized by SEM (JEOL Model JSM-IT500HR). Briefly, the samples were fixed and dehydrated before imaging. The bacteria in SEM micro-images were then color-coded (green) using MountainsMap software for ease of visualization.

Competitive Comparison Testing Results and Discussion

Surface Roughness: The Sa values of the collar surfaces of the implants are shown in Figure 27a. The Sa value of machined Ti alloy is measured ~ 0.3 – 0.4µm, which is slightly higher than that of Osseotite alloy (0.34µm). The reason is that due to the higher hardness of Ti alloy material, the machining lines are more pronounced on the collar, and the material does not etch as easily as the CP4 Ti. The mean Sa value of TiUltra of Nobel is measured the lowest around 0.15 µm, since the implant has a hybrid surface that gradually transitions into a machined surface in the collar area and due to its CP4 nature, it is smoother than machined alloy Ti surface.

However, there were no significant differences between these three surfaces. The MTX of ZimVie and SBM of Implant Direct are both grit blasted surfaces with mean Sa values of ~ 0.8µm and ~ 1µm, respectively, both significantly higher than that of Osseotite surface. TiUnite of Nobel and C1 of MIS have the mean Sa value of ~ 1.2µm, followed by Osseospeed of Dentsply and SLA of Straumann with mean Sa value around 2µm, and Laser-Lok of Biohorizons with mean Sa around 2.8µm. In summary, all the surfaces, except TiUltra and machined, had significantly higher Sa than that of Osseotite surface.

Bacterial Adhesion: The adherent live bacteria was quantified by measuring the absorbance at 450nm after the incubation of the samples in WST solution for one hour (Figure 27b). The amount of adherent bacteria to all other textured surfaces was significantly higher than Osseotite surface, except for TiUltra, machined, and MTX surfaces. These observations were in line with the results of the prior experiments using discs. While the surface roughness of MTX was significantly higher than that of Osseotite surface, there was only an insignificant increase in the amount of adherent bacteria to the MTX surface.

It was also expected to observe no differences in the amount of adherent bacteria on TiUltra, machined and Osseotite surfaces. It is noteworthy that TiUltra surface has a machined non-textured finish on the collar region and acts as a machined surface when exposed to bacteria. The results again confirmed a cut-off roughness Sa value around 1 µm, below which the textured surfaces won't favor increased bacterial adhesion.

Fig. 27a

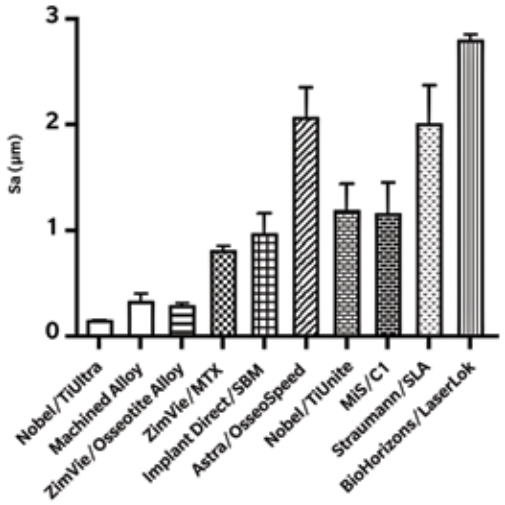

Fig. 27b

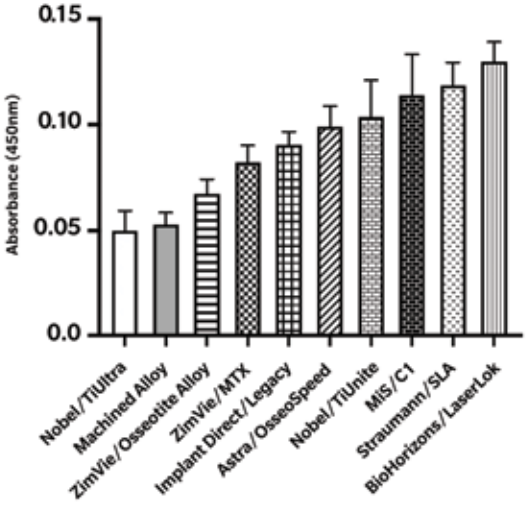

Comparisons	Summary	Adjusted P Value
TiUltra vs. Osseotite	ns	.932
Machined vs. Osseotite	ns	>.999
MTX vs. Osseotite	**	.007
SBM vs. Osseotite	***	<.001
OsseoSpeed vs. Osseotite	***	<.001
TiUnite vs. Osseotite	***	<.001
C1 vs. Osseotite	***	<.001
SLA vs. Osseotite	***	<.001
LaserLok vs. Osseotite	***	<.001

Comparisons	Summary	Adjusted P Value
TiUltra vs. Osseotite	ns	.178
Machined vs. Osseotite	ns	.364
MTX vs. Osseotite	ns	.312
SBM vs. Osseotite	*	.038
OsseoSpeed vs. Osseotite	**	.003
TiUnite vs. Osseotite	***	<.001
C1 vs. Osseotite	***	<.001
SLA vs. Osseotite	***	<.001
LaserLok vs. Osseotite	***	<.001

Fig. 27 *(a) Surface roughness of the tested implant collar surfaces reported as Sa values measured using Keyence microscope. (b) Quantification of adherent live bacteria to the collar surfaces as measured by absorbance at 450nm. NOTE: The tables below each graph list the corresponding p values.*

The adherence of bacteria to the collar of tested implants were further examined with SEM *(Figure 28)*. The qualitative findings were in line with the quantitative analysis of the adherent bacteria showing no increased bacterial adhesion to Osseotite surface compared with the machined and TiUltra surfaces. Other minimally rough (Sa: 0.5 – 1µm) and moderately rough (Sa: 1 – 2µm) surfaces had a higher amount of adherent bacteria compared to Osseotite surface, and rough (Sa > 2µm) surfaces such as Laser-Lok, and SLA were almost completely covered by the adherent bacteria. The distribution of adherent bacteria on the surfaces seems to be random. However, they are more favorably attached and continue to group around the sharp edges of the acid-etching pits, between large micron-sized grit blasted peaks, around or inside large anodized pores, and on peaks and valleys of laser channels.

SEM Images

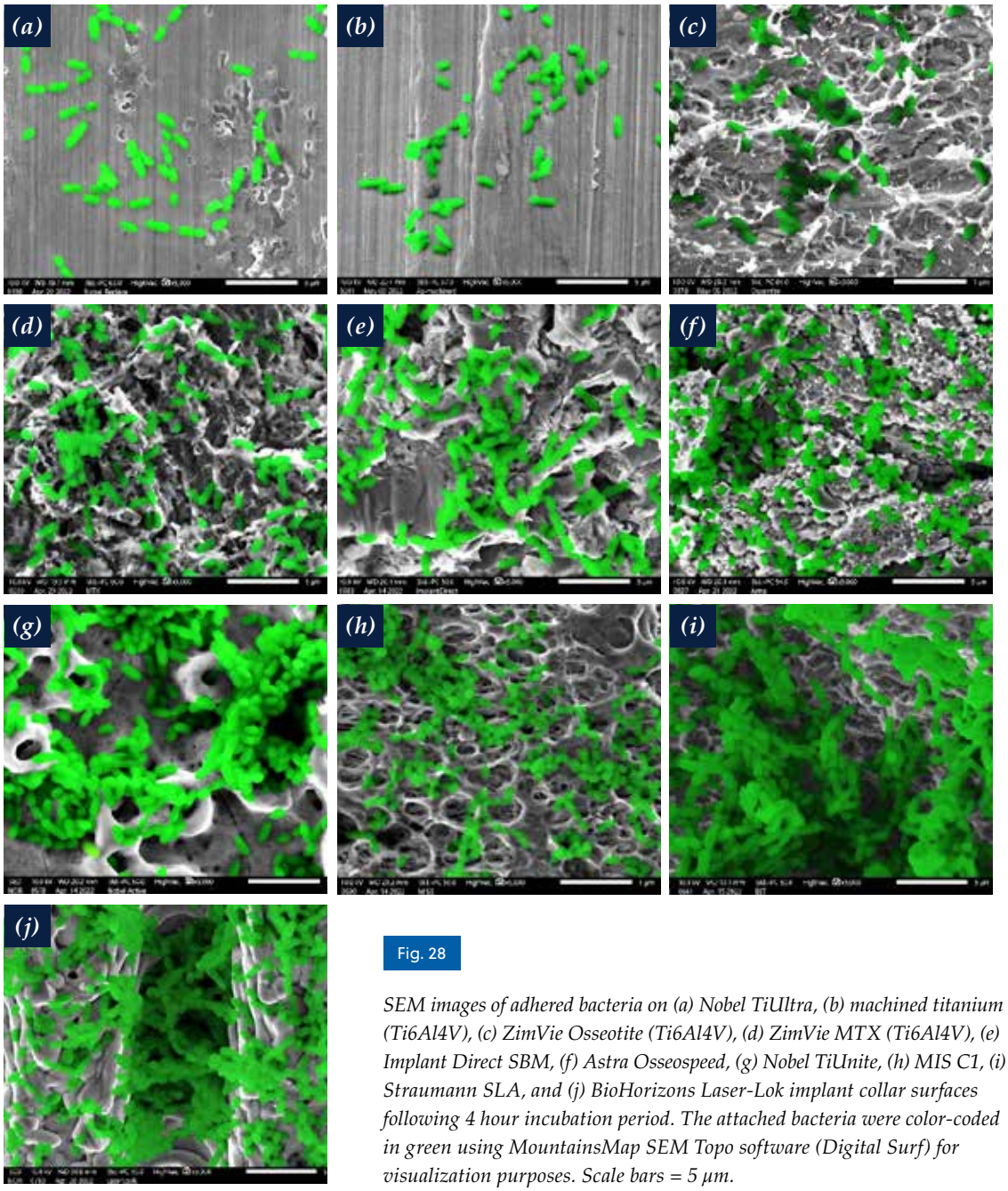

Fig. 28

SEM images of adhered bacteria on (a) Nobel TiUltra, (b) machined titanium (Ti6Al4V), (c) ZimVie Osseotite (Ti6Al4V), (d) ZimVie MTX (Ti6Al4V), (e) Implant Direct SBM, (f) Astra Osseospeed, (g) Nobel TiUnite, (h) MIS C1, (i) Straumann SLA, and (j) BioHorizons Laser-Lok implant collar surfaces following 4 hour incubation period. The attached bacteria were color-coded in green using MountainsMap SEM Topo software (Digital Surf) for visualization purposes. Scale bars = 5 µm.

Competitive Comparison Testing Conclusion

The results of this in vitro study confirmed prior findings that by applying dual acid etching on the collar of the TSX Implant, the amount of adherent bacteria is reduced compared to the traditional MTX surface but not increased compared to the machined surface. It was also confirmed that there seems to be a cut-off threshold roughness around Sa of 1µm, above which the adhesion of bacteria increases significantly, while below that, a similar bacterial adhesion profile to a machined surface is observed. Furthermore, large grooves, wide pores, and deep craters that are larger than the size of pathogenic bacteria are favored by the bacteria to accumulate, thus posing an increased risk of biofilm formation.

SUMMARY

TSX Design for Peri-Implant Health

The TSX Implant has been designed with a contemporary hybrid surface with the threaded body having the MTX surface, while the coronal 1.5 mm of the TSX Implant is textured with dual acid etching technology to balance the peri-implant tissue health and enhanced osseointegration potential of the implant in the coronal region. Both the dual acid-etched and the MTX surfaces have great osseointegration potential and proven long-term clinical success for over 20 years. Furthermore, the dual acid-etched surface has been shown to not only help in crestal bone maintenance compared to a machined surface, but also help contain the adhesion of bacteria at the level of a machined surface. Indeed, the surface Sa roughness and morphology of the dual acid-etched surface are within the range to improve the osteoconduction process without increasing the adherence of pathogenic bacteria. Therefore, it is an excellent alternative to the traditional approach using a machined surface with compromised osteoconduction potential at the coronal aspect of the implant to reduce bacterial adhesion and the risk of biofilm formation.

Moderately rough and rough coronal surfaces with Sa values higher than that of the dual acid-etched surface (Sa > 1µm) have been shown to increase the amount of adherent bacteria and may present a higher risk of peri-implantitis if exposed to the oral cavity. However, the dual acid-etched surface, if exposed, will be easier to clean and disinfect as compared to rougher surfaces. Therefore, with the dual acid-etched coronal surface, excellent osteoconduction potential is combined with reduced bacterial adhesion, resulting in the maintenance of crestal bone level and reduced risk of biofilm formation, which along with the platform switching technology and the friction-fit internal hex connection offers an exceptional peri-implant tissue health.

CONCLUSION

The TSX Implant design incorporates time-tested, clinically proven features that address both the fundamentals of implant success established in the 1990s – enhanced osseointegration and implant-abutment stability – as well as the contemporary needs for immediacy and long-term peri-implant health.

The TSX Implant also represents the integration of the best and most popular features from two scientific, clinically-focused, and industry-leading companies that merged in 2015 and now comprise ZimVie Dental, established in 2022.

Extensive pre-clinical investigation was conducted to validate the concepts utilized in the TSX Implant design to achieve high primary stability, extraction site stability, and to provide additional support for the incorporation of a hybrid surface with long-term evidence of a similar risk of peri-implantitis to machined titanium while providing better osseoconductivity and higher bone levels than machined titanium.

Preclinical testing confirms the TSX Implant has the potential for high primary stability for immediacy including immediate extraction placement as well as the potential for long-term peri-implant health. Clinical study is needed to confirm pre-clincial results, and studies will commence in 2023.

References

1. Data on File.
2. Hürzeler M, Fickl S, Zuhr O, Wachtel HC. Peri-implant bone level around implants with platform-switched abutments: preliminary data from a prospective study. J Oral Maxillofac Surg. 2007;65(7 Suppl 1):33-9.
3. Calvo Guirado JL, Saez Yuguero MR, Pardo Zamora G, Muñoz Barrio E. Immediate provisionalization on a new implant design for esthetic restoration and preserving crestal bone. Implant Dent. 2007;16(2):155-64.
4. Calvo-Guirado JL, Ortiz-Ruiz AJ, López-Marí L, Delgado-Ruiz R, Maté-Sánchez J, Bravo Gonzalez LA. Immediate maxillary restoration of single-tooth implants using platform switching for crestal bone preservation: a 12-month study. Int J Oral Maxillofac Implants. 2009;24(2):275-81.
5. Baumgarten H, Cocchetto R, Testori T, Meltzer A, Porter S. A new implant design for crestal bone preservation: initial observations and case report. Pract Proced Aesthet Dent. 2005;17(10):735-40.
6. Vela-Nebot X, Rodríguez-Ciurana X, Rodado-Alonso C, Segalà-Torres M. Benefits of an implant platform modification technique to reduce crestal bone resorption. Implant Dent. 2006;15(3):313-20.
7. Degidi M, Iezzi G, Scarano A, Piattelli A. Immediately loaded titanium implant with a tissue-stabilizing/maintaining design ('beyond platform switch') retrieved from man after 4 weeks: a histological and histomorphometrical evaluation. A case report. Clin Oral Implants Res. 2008;19(3):276-82.
8. Glibert M, Vervaeke S, De Bruyn H, Östman PO. Clinical and Radiographic Comparison between Platform-Shifted and Nonplatform-Shifted Implant: A One-Year Prospective Study. Clin Implant Dent Relat Res. 2016;18(1):129-37.
9. Duque AD, Aristizabal AG, Londoño S, Castro L, Alvarez LG. Prevalence of peri-implant disease on platform switching implants: a cross-sectional pilot study. Braz Oral Res. 2016;30.
10. Amato F, Polara G, Spedicato GA. Immediate Loading of Fixed Partial Dental Prostheses on Extra-Short and Short Implants in Patients with Severe Atrophy of the Posterior Maxilla or Mandible: An Up-to-4-year Clinical Study. Int J Oral Maxillofac Implants. 2020;35(3):607-15.
11. Hagiwara Y. Does platform switching really prevent crestal bone loss around implants? Japanese Dental Science Review 2010;46:122-31.
12. Farronato D, Manfredini M, Farronato M, Pasini PM, Orsina AA, Lops D. Behavior of Soft Tissue around Platform-Switched Implants and Non-Platform-Switched Implants: A Comparative Three-Year Clinical Study. J Clin Med. 2021;10(13).
13. Maeda Y, Miura J, Taki I, Sogo M. Biomechanical analysis on platform switching: is there any biomechanical rationale? Clin Oral Implants Res. 2007;18(5):581-4.
14. Schrotenboer J, Tsao YP, Kinariwala V, Wang HL. Effect of platform switching on implant crest bone stress: a finite element analysis. Implant Dent. 2009;18(3):260-9.
15. Binon PP. The evolution and evaluation of two interference-fit implant interfaces. Postgraduate Dent 1996;3(1):3-13.
16. Mihalko WM, May TC, Kay JF, Krause WR. Finite element analysis of interface geometry effects on the crestal bone surrounding a dental implant. Implant Dent. 1992;1(3):212-7.
17. Macedo JP, Pereira J, Vahey BR, Henriques B, Benfatti CAM, Magini RS, et al. Morse taper dental implants and platform switching: The new paradigm in oral implantology. Eur J Dent. 2016;10(1):148-54.
18. Schmitt CM, Nogueira-Filho G, Tenenbaum HC, Lai JY, Brito C, Döring H, et al. Performance of conical abutment (Morse Taper) connection implants: a systematic review. J Biomed Mater Res A. 2014;102(2):552-74.
19. Kofron MD, Carstens M, Fu C, Wen HB. In vitro assessment of connection strength and stability of internal implant-abutment connections. Clin Biomech (Bristol, Avon). 2019;65:92-9.
20. Hansson S. Implant-abutment interface: biomechanical study of flat top versus conical. Clin Implant Dent Relat Res. 2000;2(1):33-41.
21. Sullivan DY, Sherwood RL, Porter SS. Long-term performance of Osseotite implants: a 6-year clinical follow-up. Compend Contin Educ Dent. 2001;22(4):326-8, 30, 32-4.
22. Davarpanah M, Martinez H, Etienne D, Zabalegui I, Mattout P, Chiche F, et al. A prospective multicenter evaluation of 1,583 3i implants: 1- to 5-year data. Int J Oral Maxillofac Implants. 2002;17(6):820-8.
23. Feldman S, Boitel N, Weng D, Kohles SS, Stach RM. Five-year survival distributions of short-length (10 mm or less) machined-surfaced and Osseotite implants. Clin Implant Dent Relat Res. 2004;6(1):16-23.
24. Sullivan D, Vincenzi G, Feldman S. Early loading of Osseotite implants 2 months after placement in the maxilla and mandible: a 5-year report. Int J Oral Maxillofac Implants. 2005;20(6):905-12.

25. Testori T, Wiseman L, Woolfe S, Porter SS. A prospective multicenter clinical study of the Osseotite implant: four-year interim report. Int J Oral Maxillofac Implants. 2001;16(2):193-200.

26. Testori T, Del Fabbro M, Feldman S, Vincenzi G, Sullivan D, Rossi R, Jr., et al. A multicenter prospective evaluation of 2-months loaded Osseotite implants placed in the posterior jaws: 3-year follow-up results. Clin Oral Implants Res. 2002;13(2):154-61.

27. Gaucher H, Bentley K, Roy S, Head T, Blomfield J, Blondeau F, et al. A multi-centre study of Osseotite implants supporting mandibular restorations: a 3-year report. J Can Dent Assoc. 2001;67(9):528-33.

28. Stach RM, Kohles SS. A meta-analysis examining the clinical survivability of machined-surfaced and osseotite implants in poor-quality bone. Implant Dent. 2003;12(1):87-96.

29. Bain CA, Weng D, Meltzer A, Kohles SS, Stach RM. A meta-analysis evaluating the risk for implant failure in patients who smoke. Compend Contin Educ Dent. 2002;23(8):695-9, 702, 4 passim; quiz 8.

30. Lazzara RJ, Testori T, Trisi P, Porter SS, Weinstein RL. A human histologic analysis of osseotite and machined surfaces using implants with 2 opposing surfaces. Int J Periodontics Restorative Dent. 1999;19(2):117-29.

31. Zetterqvist L, Feldman S, Rotter B, Vincenzi G, Wennström JL, Chierico A, et al. A prospective, multicenter, randomized-controlled 5-year study of hybrid and fully etched implants for the incidence of peri-implantitis. J Periodontol. 2010;81(4):493-501.

32. Amoroso PF, Adams RJ, Waters MG, Williams DW. Titanium surface modification and its effect on the adherence of Porphyromonas gingivalis: an in vitro study. Clin Oral Implants Res. 2006;17(6):633-7.

33. Bermejo P, Sánchez MC, Llama-Palacios A, Figuero E, Herrera D, Sanz Alonso M. Biofilm formation on dental implants with different surface micro-topography: An in vitro study. Clin Oral Implants Res. 2019;30(8):725-34.

34. Park SJ, Sanchez O, Ajami E, Wen HB. Bacterial Adhesion to Different Dental Implant Collar Surfaces: An in-vitro comparative study Academy of Osseointegration; MARCH 13-16, 2019; Washington DC.

35. Subramani K, Jung RE, Molenberg A, Hammerle CH. Biofilm on dental implants: a review of the literature. Int J Oral Maxillofac Implants. 2009;24(4):616-26.

36. Trisi P, Marcato C, Todisco M. Bone-to-implant apposition with machined and MTX microtextured implant surfaces in human sinus grafts. Int J Periodontics Restorative Dent. 2003;23(5):427-37.

37. Todisco M, Trisi P. Histomorphometric evaluation of six dental implant surfaces after early loading in augmented human sinuses. J Oral Implantol. 2006;32(4):153-66.

38. Morris HF, Ochi S. The influence of implant design, application, and site on clinical performance and crestal bone: a multicenter, multidisciplinary clinical study. Dental Implant Clinical Research Group (Planning Committee). Implant Dent. 1992;1(1):49-55.

39. Lazzara RJ, Porter SS. Platform switching: a new concept in implant dentistry for controlling postrestorative crestal bone levels. Int J Periodontics Restorative Dent. 2006;26(1):9-17.

40. Rosenlicht JL. Advancements in soft bone implant stability. West Indian Dent J 2002;6:2-7.

41. Patil YB, Asopa SJ, Deepa, Goel A, Jyoti D, Somayaji NS, et al. Influence of Implant Neck Design on Crestal Bone Loss: A Comparative Study. Niger J Surg. 2020;26(1):22-7.

42. Doornewaard R, Christiaens V, De Bruyn H, Jacobsson M, Cosyn J, Vervaeke S, et al. Long-Term Effect of Surface Roughness and Patients' Factors on Crestal Bone Loss at Dental Implants. A Systematic Review and Meta-Analysis. Clin Implant Dent Relat Res. 2017;19(2):372-99.

43. Sicilia A, Gallego L, Sicilia P, Mallo C, Cuesta S, Sanz M. Crestal bone loss associated with different implant surfaces in the posterior mandible in patients with a history of periodontitis. A retrospective study. Clin Oral Implants Res. 2021;32(1):88-99.

44. Petrini M, Giuliani A, Di Campli E, Di Lodovico S, Iezzi G, Piattelli A, et al. The Bacterial Anti-Adhesive Activity of Double-Etched Titanium (DAE) as a Dental Implant Surface. Int J Mol Sci. 2020;21(21).

45. Kligman S, Ren Z, Chung CH, Perillo MA, Chang YC, Koo H, et al. The Impact of Dental Implant Surface Modifications on Osseointegration and Biofilm Formation. J Clin Med. 2021;10(8).

46. Fürst MM, Salvi GE, Lang NP, Persson GR. Bacterial colonization immediately after installation on oral titanium implants. Clin Oral Implants Res. 2007;18(4):501-8.

47. Roehling S, Astasov-Frauenhoffer M, Hauser-Gerspach I, Braissant O, Woelfler H, Waltimo T, et al. In Vitro Biofilm Formation on Titanium and Zirconia Implant Surfaces. J Periodontol. 2017;88(3):298-307.

For more information, visit ZimVie.com

ZimVie
4555 Riverside Drive
Palm Beach Gardens, FL 33410
1-800-342-5454
Phone: +1-561-776-6700
Fax: +1-561-776-1272

IMPLACOM
IMPLANTEREN ZONDER ZORGEN

www.implacom.nl | +31 (0)577 46 1927

ZimVie
Restoring Daily Life.®